

PREPARED FOR SUBMISSION TO JHEP

Naturally small neutrino mass with asymptotic safety and gravitational-wave signatures

Abhishek Chikkaballi, Kamila Kowalska and Enrico Maria Sessolo

*National Centre for Nuclear Research,
Pasteura 7, 02-093 Warsaw, Poland*

E-mail: abhishek.chikkaballiramalingegowda@ncbj.gov.pl,
kamila.kowalska@ncbj.gov.pl, enrico.sessolo@ncbj.gov.pl

ABSTRACT: We revisit the dynamical generation of an arbitrarily small neutrino Yukawa coupling in the Standard Model with trans-Planckian asymptotic safety and apply the same mechanism to the gauged $B - L$ model. We show that thanks to the presence of additional irrelevant couplings, the described neutrino-mass generation in the $B - L$ model is potentially more in line with existing theoretical calculations in quantum gravity. Interestingly, the model can accommodate, in full naturalness and without extensions, the possibility of purely Dirac, pseudo-Dirac, and Majorana neutrinos with any see-saw scale. We investigate eventual distinctive signatures of these cases in the detection of gravitational waves from first-order phase transitions. We find that, while it is easy to produce a signal observable in new-generation interferometers, its discriminating features are washed out by the strong dependence of the gravitational-wave spectrum on the relevant parameters of the scalar potential.

Contents

1	Introduction	1
2	General notions of asymptotic safety	4
3	Small Yukawa couplings from UV fixed points	6
3.1	General setup	6
3.2	Trans-Planckian features of neutrino mass models	8
3.3	Possible connections to the FRG	11
4	Boundary conditions of the $B - L$ model	13
4.1	Fixed points of the gauge-Yukawa system	13
4.2	Scalar potential	16
5	Gravitational waves	20
6	Conclusions	23
	Appendices	24
A	Renormalization group equations	24
B	Thermally corrected effective potential	26
C	Phase transition and gravitational waves	27

1 Introduction

A large amount of atmospheric, reactor, and accelerator data have robustly shown that neutrinos have a mass, and that their mass is much smaller than the masses of the other fermions of the Standard Model (SM). If (Dirac) neutrino masses were generated via the Higgs mechanism, they would require a minuscule Yukawa coupling, of the order of 10^{-13} , lower by several orders of magnitude than the other SM Yukawa couplings, which range between $\sim 10^{-5}$ and 1. To deal with such uncomfortably and potentially unnaturally small values, numerous new physics (NP) constructions have been developed in recent decades with the goal of dynamically generating the neutrino mass. Perhaps the most famous of those constructions is the see-saw mechanism [1–7], although radiative models also lend a popular alternative, see, *e.g.*, Refs. [8, 9] for reviews.

Recently [10] (see also [11]), some of us proposed yet another way of obtaining dynamically a naturally small neutrino mass, which does not have to be suppressed by a large

Majorana scale, like in the see-saw mechanism, nor is it parameterized by the small spontaneous breaking of lepton-number symmetry, like in the inverse see-saw model [12–14]. In Ref. [10], the trans-Planckian renormalization group (RG) flow of the neutrino Yukawa coupling develops a Gaussian infrared (IR)-attractive fixed point. The neutrino can naturally be a Dirac particle, because its Yukawa coupling will be exponentially suppressed. In the SM with the addition of three right-handed neutrinos (SMRHN) it was shown that such a mechanism is consistent with all low-energy data on neutrino masses and mixing and that it favors the normal, rather than inverted, hierarchical ordering.

The construction of Ref. [10] finds its motivation in the vast body of work pointing to the existence of asymptotically safe quantum gravity. Asymptotic safety (AS) is the property of a quantum field theory to develop fixed points of the RG flow of the action [15]. Following the development of functional renormalization group (FRG) techniques a few decades ago [16, 17], it was shown in several papers that AS can arise quite naturally in quantum gravity and provide the key ingredient for the non-perturbative renormalizability of the theory. Fixed points were identified initially for the rescaled Newton coupling and the cosmological constant in the Einstein-Hilbert truncation of the effective action [18–20], and later confirmed in the presence of gravitational operators of increasing mass dimension [21–29], and of matter-field operators [30–32].

The properties of asymptotically safe quantum gravity may also influence particle physics in four space-time dimensions, as not only the gravitational action but the full system of gravity and matter may feature ultraviolet (UV) fixed points in the energy regime where gravitational interactions become strong [33–44]. A trans-Planckian fixed point may thus induce some specific boundary conditions for some of the *a priori* free couplings of the matter Lagrangian, as long as they correspond to *irrelevant* directions in theory space. Early “successes” of AS applied to particle physics are a gravity-driven solution to the triviality problem in U(1) gauge theories [45–47]; a ballpark prediction for the value of the Higgs mass (more precisely, of the quartic coupling of the Higgs potential) obtained a few years ahead of its discovery [48] (see also Refs. [49–51]); and the retroactive “postdiction” of the top-mass value [52].

The simple ingredient beneath the construction of Ref. [10] is that the trans-Planckian renormalization group equations (RGEs) should accommodate a negative critical exponent for the Gaussian fixed point of the neutrino Yukawa coupling. Such a feature should ideally emerge from a first-principle calculation based on the FRG. It turns out, however, that at least in the SMRHN it may not be easy to obtain full consistency between the quantum-gravity calculation and a phenomenologically viable neutrino-mass generation. The reason ultimately lies in an inherent lack of free couplings in the matter theory.

Let us clarify this point by recalling that the effects of gravity on the SM Yukawa RGEs are universal, so that they cannot be responsible for any qualitative behavior differentiating one type of Yukawa coupling from the others. In other words, any feature specific to the neutrino Yukawa coupling (but not shared by the others) must be driven by the SM-like terms of the trans-Planckian RGEs, rather than by effects originating in the purely gravitational action. As we shall see in Sec. 3, the non-interactive IR-attractive fixed point of the neutrino Yukawa coupling can only be reached in the SMRHN in the presence

of an interactive IR-attractive fixed point of the hypercharge gauge coupling g_Y . Since the value of the hypercharge coupling is very well measured at low energy, a first-principle calculation based on the FRG would have to produce an extremely precise desired outcome or otherwise spoil the entire low-energy phenomenology.

The problem just described can be avoided by replacing the dynamical “pull” exerted on the RG flow by the IR-attractive hypercharge fixed point with an equivalent effect due to other couplings that are not well-measured yet, trading thus a constraint for a prediction. We consider in this paper perhaps the simplest and most natural extension of the SMRHN, the well-known gauged $B - L$ model [53, 54], which extends the SM gauge group with an abelian $U(1)_{B-L}$ symmetry. The gauge coupling g_{B-L} and kinetic mixing g_ϵ can generate a negative critical exponent for the neutrino Yukawa coupling in the same way as g_Y does in the SMRHN.

Being anomaly-free, the $B - L$ model naturally accommodates the three right-handed neutrino spinor fields. By only featuring gauge symmetries, moreover, it allows one to bypass problems potentially associated with continuous global symmetries in quantum gravity.¹ The $B - L$ model also allows for the generation of a Majorana mass term from spontaneous symmetry breaking. Such a feature may seem to blunt the need for a dynamical mechanism alternative to the see-saw. However, we will show that pseudo-Dirac and even fully Dirac neutrino masses can naturally emerge when the $B - L$ model is embedded in AS.

Finally, by being endowed with a NP scalar field, the model provides a natural framework for the spontaneous generation of intermediate scales, either directly or via dimensional transmutation with the Coleman-Weinberg mechanism [58]. Assuming the latter applies, it is then interesting to compute potential gravitational-wave (GW) signatures from first-order phase transitions (FOPTs) [59–62] (see also Ref. [63] for a recent comprehensive review). We investigate them in this work, with the ultimate hope of associating some of their features to the dynamical generation of a Majorana or a Dirac neutrino mass in the context of AS.

The paper is organized as follows. In Sec. 2 we review some general notions of trans-Planckian AS, which is the framework we adopt for our neutrino-mass generation mechanism. The details of this mechanism are recalled in Sec. 3, where we show that it applies equally well to the SMRHN and the gauged $B - L$ model. We also discuss the obstacles one encounters when confronting the former with an asymptotically safe UV completion based on quantum gravity. The trans-Planckian boundary conditions of the $B - L$ model are given in Sec. 4, where we also discuss the scalar potential. GW signatures from FOPTs are investigated in Sec. 5. Finally, we derive our conclusions in Sec. 6. Appendices are dedicated to the explicit form of the RGEs, the explicit form of the thermally corrected effective potential, and a brief review of the GW generation from FOPTs.

¹There are indications that asymptotically safe gravity preserves global symmetries, at least under all the truncations investigated in the context of the FRG [44]. An apparent discrepancy with general arguments pointing to the violation of global symmetries in quantum gravity might be resolved in AS by the existence of black hole remnants [55], which may potentially provide protection against the disappearance of conserved global charges [56, 57].

2 General notions of asymptotic safety

The scale-dependence of all Lagrangian couplings is encoded in the RG flow. In AS, quantum gravity effects kick in at about the Planck scale, where the flow of the gravitational action develops dynamically a fixed point. Let us consider a (renormalizable) matter theory with gauge and Yukawa interactions. The RGEs receive modifications above the Planck scale that look like

$$\frac{dg_i}{dt} = \beta_i^{(\text{matter})} - f_g g_i \quad (2.1)$$

$$\frac{dy_j}{dt} = \beta_j^{(\text{matter})} - f_y y_j, \quad (2.2)$$

where we indicate the renormalization scale with $t = \ln \mu$, g_i and y_j (with $i, j = 1, 2, 3 \dots$) are the set of gauge and Yukawa couplings, respectively, and the original beta functions (without gravity) are indicated schematically with $\beta_{i,j}^{(\text{matter})}$.

The trans-Planckian gravitational corrections f_g and f_y are universal, in the sense that they multiply linearly all matter couplings of the same kind, in agreement with the expectation that gravity should not distinguish the internal degrees of freedom of the matter theory. The f_g and f_y coefficients depend on the fixed points of the operators of the gravitational action, and can be computed using the techniques of the FRG. Their computation is subject to extremely large uncertainties, which relate to the choice of truncation in the gravity/matter action, to the selected renormalization scheme, to the gauge-fixing parameters, and other effects [20, 21, 26, 64–70]. A generic functional form for f_g and f_y is (and is possibly bound to remain) unknown. What is established with some confidence is that f_g is likely not negative, irrespective of the chosen RG scheme [32, 42]. This is encouraging, as $f_g > 0$ will preserve asymptotic freedom in the non-abelian gauge sector of the SM. No fundamental constraints currently apply instead to the leading-order gravitational term f_y . The gravitational contribution to the Yukawa coupling was investigated in a set of simplified models [30, 38, 39, 43], but no general results and definite conclusions regarding the size and sign of f_y are available (but see Ref. [71] for the most recent determination of f_y in the SM).

Explicit forms of f_g and f_y exist in the literature. To give but one example, it was found in Refs. [47, 52] that, for a theory with gauge and Yukawa couplings in the matter Lagrangian, an FRG calculation in the Einstein-Hilbert truncation of the gravity action, with Litim-type regulator and $\alpha = 0, \beta = 1$ gauge-fixing choice, yields

$$f_g = \tilde{G}^* \frac{1 - 4\tilde{\Lambda}^*}{4\pi (1 - 2\tilde{\Lambda}^*)^2}, \quad f_y = -\tilde{G}^* \frac{96 + \tilde{\Lambda}^* (-235 + 103\tilde{\Lambda}^* + 56\tilde{\Lambda}^{*2})}{12\pi (3 - 10\tilde{\Lambda}^* + 8\tilde{\Lambda}^{*2})^2}, \quad (2.3)$$

where $\tilde{\Lambda} = \Lambda/\mu^2$, $\tilde{G} = G\mu^2$ are the dimensionless cosmological and Newton constant, which parameterize the Einstein-Hilbert action, and we have indicated the trans-Planckian (interactive) fixed-point values with an asterisk.

A trans-Planckian fixed point of the system of Eqs. (2.1) and (2.2) is a set $\{g_i^*, y_j^*\}$, corresponding to a zero of the beta functions: $\beta_{i(j)}^{(\text{matter})}(g_i^*, y_j^*) - f_{g(y)} g_i^*(y_j^*) = 0$. The

RGEs of couplings $\{\alpha_k\} \equiv \{g_i, y_j\}$ are then linearized around the fixed point to derive the stability matrix M_{ij} , which is defined as

$$M_{ij} = \partial\beta_i/\partial\alpha_j|_{\{\alpha_k^*\}}. \quad (2.4)$$

Eigenvalues of the stability matrix define the opposite of critical exponents θ_i , which characterize the power-law evolution of the matter couplings in the vicinity of the fixed point. If θ_i is positive, the corresponding eigendirection is dubbed as *relevant* and UV-attractive. All RG trajectories along this direction will asymptotically reach the fixed point and, as a consequence, a deviation of a relevant coupling from the fixed point introduces a free parameter in the theory (this freedom can be used to adjust the coupling at the high scale so that it matches an eventual measurement at the low scale). If θ_i is negative, the corresponding eigendirection is dubbed as *irrelevant* and IR-attractive. There exists in this case only one trajectory that the coupling’s flow can follow in its run to the low scale, thus potentially providing a clear prediction for its value at the experimentally accessible scale. Finally, $\theta_i = 0$ corresponds to a *marginal* eigendirection. The RG flow along this direction is logarithmically slow and one ought to go beyond the linear approximation provided by the stability matrix to decide whether a fixed point is UV-attractive or IR-attractive.

For the purposes of this paper, it is enough to work with $\beta_{i,j}^{(\text{matter})}$ at one loop. A thorough quantitative analysis of the uncertainties introduced by neglecting higher-order contributions was performed in Ref. [72]. It was shown there that such uncertainties remain very small, especially when considering couplings that are perturbative along the entire RG flow.

Note also that at the first order in perturbation theory the parameters of the scalar potential somewhat “decouple” from the gauge-Yukawa system, as they can only affect Eq. (2.1) from the third-loop level up, and Eq. (2.2) from the second loop. An expression similar to Eqs. (2.1) and (2.2) potentially applies to the quartic couplings of the scalar potential as well, with the gravitational corrections parameterized as f_λ . However, whether gravitational corrections to the running couplings of the scalar potential are multiplicative or not remains a model-dependent issue, as some truncations of the gravitational action can generate additive contributions to the matter beta functions of the scalar potential [73]. We will come back to the detailed analysis of the scalar potential of the $B - L$ model in the context of AS in Sec. 4.

We close this section recalling that predictions from trans-Planckian AS in particle physics systems have been investigated in depth in many recent papers. Reference [74] attempted to extract a gravity-driven prediction of the top/bottom mass ratio of the SM. Possible imprints of asymptotically safe quantum gravity in the flavor structure of the SM and, in particular, the Cabibbo-Kobayashi-Maskawa matrix, were sought in Ref. [75]. An equivalent analysis for the Pontecorvo-Maki-Nakagawa-Sakata (PMNS) matrix elements can be found in Ref. [10]. The impact of asymptotically safe quantum-gravity calculations on the RGEs of the Majorana mass term was investigated in detail in Refs. [76–78]. Predictions were also extracted for several NP models in relation to neutrino masses [79], flavor anomalies [80, 81], the muon anomalous magnetic moment [82], the relic abundance of dark matter [73, 82, 83], baryon number [84, 85], as well as axion models [86] and GWs [87].

3 Small Yukawa couplings from UV fixed points

3.1 General setup

In a gauge-Yukawa theory embedded in trans-Planckian AS, it is possible to concoct a dynamical mechanism that makes some Yukawa couplings naturally small [10, 11]. If there exists an IR-attractive, Gaussian fixed point for those Yukawa couplings, their flow from a different, UV-attractive fixed point will asymptotically tend to zero as they approach the Planck scale from above.

We exemplify this pattern by considering a simple generic system of matter RGEs, comprising one (abelian) gauge coupling g_Y , and two Yukawa couplings, y_X and y_Z . In the deep trans-Planckian regime the system takes the form of Eqs. (2.1) and (2.2),

$$\frac{dg_Y}{dt} = \frac{b_Y}{16\pi^2} g_Y^3 - f_g g_Y \quad (3.1)$$

$$\frac{dy_X}{dt} = \frac{y_X}{16\pi^2} [\alpha_X y_X^2 + \alpha_Z y_Z^2 - \alpha_Y g_Y^2] - f_y y_X \quad (3.2)$$

$$\frac{dy_Z}{dt} = \frac{y_Z}{16\pi^2} [\alpha'_X y_X^2 + \alpha'_Z y_Z^2 - \alpha'_Y g_Y^2] - f_y y_Z, \quad (3.3)$$

where $b_Y, \alpha_X^{(l)}, \alpha_Y^{(l)}, \alpha_Z^{(l)} \geq 0$ are one-loop coefficients. The reader may think of Eqs. (3.1)-(3.3) as the system of hypercharge/top Yukawa/neutrino Yukawa coupling in the SMRHN, after all other couplings have been set to their (UV-attractive) Gaussian fixed point. The discussion however is generic and can be applied to any gauge-Yukawa system [10].

Let us set the beta functions to zero and select a solution where y_Z develops a Gaussian fixed point, $y_Z^* = 0$. We expect such solution to be IR-attractive, which means that the corresponding critical exponent θ_Z should be negative:

$$16\pi^2 \theta_Z \approx -(\alpha'_X y_X^{*2} - \alpha'_Y g_Y^{*2} - 16\pi^2 f_y) < 0. \quad (3.4)$$

Equation (3.4) imposes a condition on the quantum gravity parameter f_y [10].

On the other hand, the system (3.1)-(3.3) may also feature a predictive (irrelevant) fixed point $y_X^* \neq 0$. This means that one could follow the unique trajectory of $y_X(t)$ to the low energy and extract its value at the electroweak symmetry-breaking (EWSB) scale. If y_X is then a SM Yukawa coupling, the overall consistency of the AS framework implies that f_y can only assume those specific values allowing y_X^* to be in agreement with a low energy determination of $y_X(t)$. In other words, in Eq. (3.4) one can trade f_y , which should emerge from a calculation with the FRG, with y_X^* , which should be consistent, within uncertainties, with low energy observations. We get

$$16\pi^2 \theta_Z \approx -(\alpha_Y - \alpha'_Y) g_Y^{*2} + (\alpha_X - \alpha'_X) y_X^{*2}. \quad (3.5)$$

If y_X and y_Z represent, respectively, the top quark and neutrino Yukawa couplings in the SMRHN, one finds $\alpha_Y > \alpha'_Y$, $\alpha_X > \alpha'_X$ (see, *e.g.*, Appendix A of Ref. [10]), so that Eq. (3.5) can only be negative if $g_Y^* \neq 0$.

The dynamical flow of $y_Z(t)$ towards the trans-Planckian IR can finally be extracted by integrating Eq. (3.3). After replacing $f_y \rightarrow (\alpha_X y_X^{*2} - \alpha_Y g_Y^{*2})/16\pi^2$, $y_Z(t)$ is expressed

in terms of y_X^* and g_Y^* , plus an arbitrary constant κ setting the boundary condition at the Planck scale. One gets

$$y_Z(t, \kappa) = \left[\frac{c_Y g_Y^{*2} - c_X y_X^{*2}}{e^{-(c_Y g_Y^{*2} - c_X y_X^{*2})(t/8\pi^2 - 2\kappa)} + \alpha'_Z} \right]^{1/2}, \quad (3.6)$$

where we have defined $c_Y = \alpha_Y - \alpha'_Y$ and $c_X = \alpha_X - \alpha'_X$. Imposing $\theta_Z < 0$ in Eq. (3.5) implies that $y_Z(t, \kappa)$ is monotonically increasing with t in the trans-Planckian regime, and that its value at the Planck scale is set by its “distance” from $16\pi^2\kappa$. As expected, y_Z can reach arbitrarily small values without fine tuning, being parameterized exclusively by the integration constant κ .

The mechanism just described applies to any gauge-Yukawa particle physics model embedded in asymptotically safe quantum gravity, as long as the corresponding RGEs take the form of Eqs. (3.1)-(3.3). In the SMRHN this mechanism can give rise to a Dirac neutrino mass without fine tuning after EWSB. Moreover, the asymptotically safe SMRHN turns out to be consistent with all the existing data on mass-squared differences and mixing angles, if the normal ordering of neutrino masses is assumed [10].

Some concerns may arise when pondering the consistency of this mechanism with quantum-gravity calculations of f_g and f_y based on the FRG and this is particularly true in the SMRHN. Let us recall that by imposing $g_Y^* \neq 0$ along an irrelevant direction – as we did below Eq. (3.5) – we imply that the RG flow of $g_Y(t)$, followed from the fixed point down to low energies, yields a specific prediction for the hypercharge gauge coupling. This requires in turn that only one value of f_g is allowed to emerge from the FRG calculation:

$$f_g \approx \frac{b_Y g_Y^{*2}(M_{\text{Pl}})}{16\pi^2}. \quad (3.7)$$

The numerical value of Eq. (3.7) ought to be computed very precisely, more precisely than f_y since the uncertainties on the experimental determination of g_Y are smaller than those on, *e.g.*, the \overline{MS} value of $y_t(M_t)$ and other Yukawa couplings. Even considering that FRG calculations are marred by large theoretical uncertainties, it may seem exceedingly constraining that such a specific outcome ought to emerge from the deep UV construction.

A simple way out comes from generalizing the dynamical generation of small Yukawa couplings to models less dependent on precisely measured quantities. This allows us to modify the system of Eqs. (3.1)-(3.3) in two possible ways. One can either add some extra irrelevant gauge couplings to the system, one can add extra Yukawa couplings, or both. Adding additional gauge couplings, $g_{i=1,2,3\dots}$, will induce a straightforward modification of Eq. (3.5),

$$16\pi^2\theta_Z \approx - \sum_{i,j=1,2,3\dots} (\alpha_{ij} - \alpha'_{ij}) g_i^* g_j^* + (\alpha_X - \alpha'_X) y_X^{*2}, \quad (3.8)$$

with new coefficients $\alpha_{ij}^{(l)}$. One may thus select a fixed point with a UV attractive $g_Y^* = 0$ to let the hypercharge gauge coupling effectively become a free parameter of the system. The results of an FRG computation of f_g will not need to be correlated with the $g_Y(M_t)$ value at low energies, and instead will provide some welcome predictions for NP couplings that have not been measured yet.

Alternatively, one may add to Eqs. (3.1)-(3.3) the beta function of an extra Yukawa coupling, y_W , which will develop an irrelevant interactive fixed point, $y_W^* \neq 0$. The RGE system thus becomes

$$\frac{dg_Y}{dt} = \frac{b_Y}{16\pi^2} g_Y^3 - f_g g_Y \quad (3.9)$$

$$\frac{dy_X}{dt} = \frac{y_X}{16\pi^2} [\alpha_X y_X^2 + \alpha_Z y_Z^2 + \alpha_W y_W^2 - \alpha_Y g_Y^2] - f_y y_X \quad (3.10)$$

$$\frac{dy_Z}{dt} = \frac{y_Z}{16\pi^2} [\alpha'_X y_X^2 + \alpha'_Z y_Z^2 + \alpha'_W y_W^2 - \alpha'_Y g_Y^2] - f_y y_Z \quad (3.11)$$

$$\frac{dy_W}{dt} = \frac{y_W}{16\pi^2} [\alpha''_X y_X^2 + \alpha''_Z y_Z^2 + \alpha''_W y_W^2 - \alpha''_Y g_Y^2] - f_y y_W, \quad (3.12)$$

with new available parameters $\alpha''_X, \alpha''_Y, \alpha''_Z, \alpha''_W > 0$. Selecting a fixed point with $g_Y^* = 0$, will imply a modification of Eq. (3.5):

$$16\pi^2 \theta_Z \approx - \frac{\alpha''_W (\alpha_X - \alpha'_X) + \alpha_W (\alpha'_X - \alpha''_X) + \alpha'_W (\alpha''_X - \alpha_X)}{\alpha_W - \alpha''_W} y_X^{*2}. \quad (3.13)$$

Equation (3.13) can be made negative, given appropriate coefficients in Eq. (3.12). As before, the results of the FRG calculation of f_g will cease to be correlated with known values, and one obtains a prediction for y_W^* that can be tested in future experiments.

As was anticipated in Sec. 1, both solutions are implemented straightforwardly if instead of the SMRHN one embeds the gauged $B - L$ model in trans-Planckian AS.

3.2 Trans-Planckian features of neutrino mass models

Let us briefly summarize in this subsection the features of the SMRHN and the gauged $B - L$ model, showing that both constructions give rise to equivalent predictions for the neutrino Yukawa coupling.

The SMRHN The SM is enriched with three Weyl spinors, $\nu_{R,i=1,2,3}$, that are singlets under the gauge symmetry group. The Yukawa part of the Lagrangian features a set of new Yukawa couplings,

$$\mathcal{L}_D = -y_\nu^{ij} \nu_{R,i} (H^c)^\dagger L_j + \text{H.c.}, \quad (3.14)$$

where L_j , and H are the SM lepton and Higgs boson $\text{SU}(2)_L$ doublets, $H^c \equiv i\sigma_2 H^*$ is the charged conjugate doublet, and a sum over SM generations is implied. The new Yukawa term does not violate lepton-number symmetry and the left-handed neutrino component of L_i can be combined with a right-handed counterpart, $\nu_{R,i}^\dagger$, to form three Dirac fermions once the Higgs field develops its vev, v_H , upon EWSB. The Dirac mass is generated through the Higgs mechanism as $m_D \sim y_\nu v_H / \sqrt{2}$.

Since the right-handed neutrinos are singlets of the SM gauge group, they may additionally acquire a Majorana mass,

$$\mathcal{L}_M = -\frac{1}{2} M_N^{ij} \nu_{R,i} \nu_{R,j} + \text{H.c.}, \quad (3.15)$$

which violates the conservation of lepton number and can be forbidden if the latter is promoted to being a symmetry of the theory. A possibly more natural alternative to

the Dirac-type generation of neutrino masses is thus the see-saw mechanism [1–7]. In its simplest formulation, Type-I, one obtains the well-known neutrino mass matrix by combining Eq. (3.14) and Eq. (3.15):

$$m_\nu = \begin{pmatrix} 0 & m_D^T \\ m_D & M_N \end{pmatrix}. \quad (3.16)$$

If the eigenvalues of the Majorana mass matrix M_N are much larger than typical m_D values, the diagonalization of m_ν leads to three light Majorana neutrinos with mass $\sim y_\nu^2 v_H^2 / (\sqrt{2} M_N)$, and heavy Majorana neutrinos with mass $\sim M_N$. The full set of gauge and Yukawa RGEs of the SMRHN – including the PMNS matrix elements – can be found, *e.g.*, in Appendix A of Ref. [10].

In the context of trans-Planckian AS, the eventual size of f_y effectively selects one or the other type of neutrino mass generation (Dirac or Majorana), thus creating an interesting link with the quantum gravity computation. Referring to Eq. (3.4), let us select $\alpha'_{X=t} = 3$, $\alpha'_Y = 3/4$ and have $y_{X=t}^* \neq 0$ belong to the range consistent with the low-energy determination of the top pole mass.² Then, $f_y \lesssim 8.2 \times 10^{-4}$ is required to get the critical exponent $\theta_Z < 0$ and one generates an arbitrarily small Yukawa coupling $y_{Z=\nu}$ following its trans-Planckian flow towards an IR-attractive Gaussian fixed point, cf. Eq. (3.6). The corresponding RG flow is shown in Fig. 1(a). One might say that a first-principle calculation yielding f_y in the range above will naturally favor the presence of Dirac and/or pseudo-Dirac neutrinos, or even Majorana neutrinos with a low see-saw scale. Note that, in order for this behavior to take place, it is also necessary that $f_g = 0.0097$ to a very good approximation, cf. Eq. (3.7) with $g_Y^*(M_{\text{Pl}}) = 0.47$ (at one loop) and the discussion of Sec. 3.1.

Conversely, $f_y > 8.2 \times 10^{-4}$ will lead to $\theta_Z > 0$ in Eq. (3.4), *i.e.*, a relevant $y_\nu^* = 0$. One also finds an irrelevant (predictive) $y_\nu^* \neq 0$ which is $\mathcal{O}(1)$ in size [10], thus favoring a Majorana neutrino with a high see-saw scale.

Gauged $B - L$ model The SM symmetry is extended by an abelian gauge group $U(1)_{B-L}$, with gauge coupling g_{B-L} . The particle content is extended with a SM-singlet complex scalar field S , whose vev v_S spontaneously breaks $U(1)_{B-L}$. The abelian charges of the SM and NP fields can be found, *e.g.*, in Refs. [88, 89].

The Yukawa part of the Lagrangian includes Eq. (3.14), whereas Eq. (3.15) is replaced by

$$\mathcal{L}_M = -y_N^{ij} S \nu_{R,i} \nu_{R,j} + \text{H.c.}, \quad (3.17)$$

in terms of a new Yukawa coupling matrix in flavor space, y_N^{ij} . The vev v_S generates the Majorana mass upon spontaneous breaking of $U(1)_{B-L}$. As we shall see in Sec. 4.2, $v_S \gg v_H$, so that one can work in the basis where the Majorana mass is diagonal. If the boundary conditions from AS require that they are irrelevant, all three diagonal couplings will be equal, $y_N^{ii} \equiv y_N$.

² In Ref. [10] this was loosely determined to be $0.94 \lesssim y_t(M_t) \lesssim 1$, leading to $-10^{-4} \lesssim f_y \lesssim 10^{-3}$.

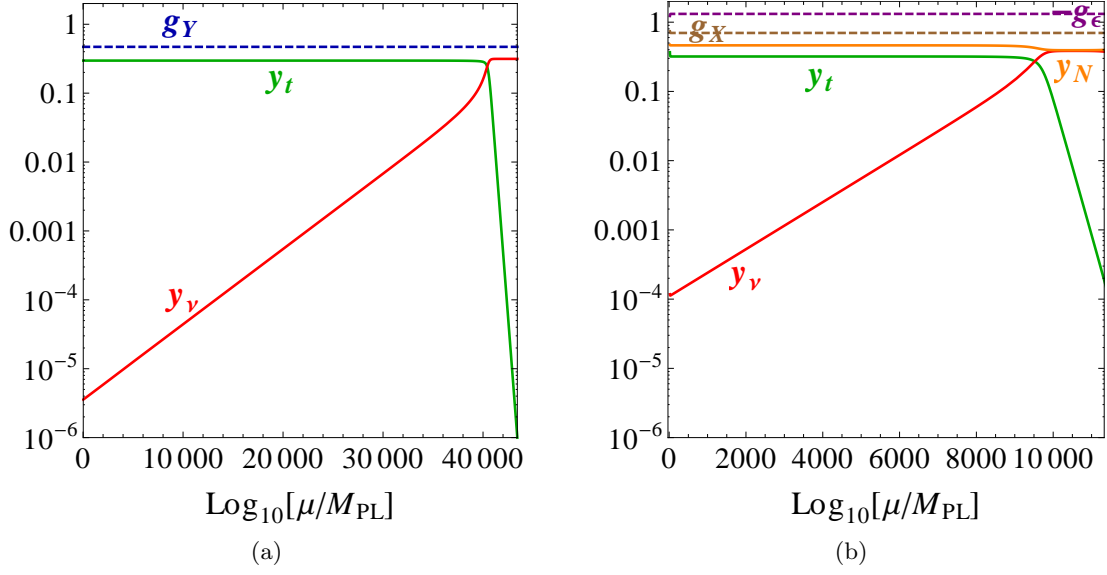


Figure 1: (a) An example of trans-Planckian trajectories for the RGE system composed of g_Y (blue, dashed), y_t (green, solid), and y_ν (red, solid) in the SMRHN with $f_g = 0.0097$, $f_y = 0.0005$. Neutrino Yukawa coupling y_ν can be made arbitrarily small at the Planck scale by adjusting the integration constant κ in Eq. (3.6). (b) The same in the gauged $B-L$ model. We set $f_g = 0.05$ and $f_y = -0.005$. Besides y_ν and y_t , we plot the trans-Planckian flow of g_X (brown, dashed), $-g_\epsilon$ (purple, dashed) and y_N (orange, solid). Note that g_Y (not shown) is here a relevant parameter.

The abelian gauge part of the Lagrangian takes the form

$$\mathcal{L} \supset -\frac{1}{4}B_{\mu\nu}B^{\mu\nu} - \frac{1}{4}X_{\mu\nu}X^{\mu\nu} - \frac{\epsilon}{2}B_{\mu\nu}X^{\mu\nu} + i\bar{f}\left(\partial^\mu - ig_Y Q_Y \tilde{B}^\mu - ig_{B-L} Q_{B-L} \tilde{X}^\mu\right)\gamma_\mu f, \quad (3.18)$$

where \tilde{B}^μ and \tilde{X}^μ are the gauge bosons of $U(1)_Y$ and $U(1)_{B-L}$, respectively, and $B_{\mu\nu}$ and $X_{\mu\nu}$ are the corresponding field strength tensors. Kinetic mixing ϵ is typically generated between the two abelian groups, as SM fermions f transform under both symmetry factors with charges Q_Y , Q_{B-L} .

It is convenient to work in a basis in which the gauge fields are canonically normalized. This is typically achieved by a rotation [90, 91]

$$\begin{pmatrix} \tilde{B}^\mu \\ \tilde{X}^\mu \end{pmatrix} = \begin{pmatrix} 1 & -\epsilon/\sqrt{1-\epsilon^2} \\ 0 & 1/\sqrt{1-\epsilon^2} \end{pmatrix} \begin{pmatrix} V^\mu \\ D^\mu \end{pmatrix}, \quad (3.19)$$

which parameterizes the gauge interaction vertices of Lagrangian (3.18) in terms of a SM gauge boson V^μ and a NP gauge boson D^μ :

$$(Q_Y, Q_{B-L}) \begin{pmatrix} g_Y & 0 \\ 0 & g_{B-L} \end{pmatrix} \begin{pmatrix} \tilde{B}^\mu \\ \tilde{X}^\mu \end{pmatrix} \rightarrow (Q_Y, Q_{B-L}) \begin{pmatrix} g_Y & g_\epsilon \\ 0 & g_X \end{pmatrix} \begin{pmatrix} V^\mu \\ D^\mu \end{pmatrix}. \quad (3.20)$$

The elements g_Y , g_X , and g_ϵ are related to the original couplings as

$$g_Y \rightarrow g_Y, \quad g_X = \frac{g_{B-L}}{\sqrt{1-\epsilon^2}}, \quad g_\epsilon = -\frac{\epsilon g_Y}{\sqrt{1-\epsilon^2}}. \quad (3.21)$$

The RGEs of the gauged $B-L$ model are given at one loop in Appendix A. One can refer to Eq. (3.8) and Eq. (3.13), with appropriate numerical coefficients, to show that the RG flow of the neutrino Yukawa coupling admits a Gaussian irrelevant fixed point driven by the irrelevant fixed points of new gauge and Yukawa couplings, $g_X^* \neq 0$, $g_\epsilon^* \neq 0$, and $y_N^* \neq 0$. We show the trans-Planckian flow of the couplings in Fig. 1(b). Note that the behavior of y_ν mimics exactly the SMRHN case, while g_Y can originate from a relevant fixed point and remain free independently of the value of f_g .

3.3 Possible connections to the FRG

The freedom of adjusting the value of f_g arbitrarily without spoiling the dynamical generation of a small neutrino Yukawa coupling becomes valuable when confronting the phenomenologically viable parameter space with existing computations from the FRG. As was discussed in Sec. 2, calculations of f_g and f_y from first principles are marred by large theory uncertainties [20, 21, 26, 64–70]. We can nonetheless refer to some of the explicit existing cases in the literature and make the point that, even considering those uncertainties, the $B-L$ model likely provides a more flexible framework than the SMRHN to match a UV calculation with the low-scale phenomenology.

Let us return to the explicit f_g , f_y computations of Refs. [47, 52], which were recalled in Eq. (2.3). In Fig. 2(a) we show in the $(\tilde{\Lambda}^*, \tilde{G}^*)$ plane the parameter space consistent with the generation of a small neutrino Yukawa coupling and phenomenological constraints in the SMRHN. The solid blue line corresponds to $f_g = 0.0097$, cf. Eq. (3.7), and the shaded (orange) region corresponds to the requirement of having the correct top mass, cf. footnote 2.

Fixed point values $(\tilde{\Lambda}^*, \tilde{G}^*)$ are zeros of the gravity beta functions, which are computed with FRG techniques. In the Einstein-Hilbert truncation and $\beta = 1, \alpha = 0$ gauge, they read [47]

$$\frac{d\tilde{G}}{dt} = 2\tilde{G} + \frac{\tilde{G}^2}{6\pi} (2N_D + N_S - 4N_V) - \frac{\tilde{G}^2}{6\pi} \left(14 + \frac{6}{1-2\tilde{\Lambda}} + \frac{9}{(1-2\tilde{\Lambda})^2} \right) \quad (3.22)$$

$$\begin{aligned} \frac{d\tilde{\Lambda}}{dt} = & -2\tilde{\Lambda} + \frac{\tilde{G}}{4\pi} (N_S - 4N_D + 2N_V) + \frac{\tilde{G}\tilde{\Lambda}}{6\pi} (N_S + 2N_D - 4N_V) - \frac{3\tilde{G}}{2\pi} - \frac{7\tilde{G}\tilde{\Lambda}}{3\pi} \\ & + \frac{7\tilde{G}}{4\pi(1-2\tilde{\Lambda})} - \frac{3\tilde{G}}{4\pi(1-2\tilde{\Lambda})^2}. \end{aligned} \quad (3.23)$$

Equations (3.22) and (3.23) depend on the number of matter fields in the theory: real scalars (N_S), Dirac fermions (N_D), and vector gauge bosons (N_V). In the SMRHN, $N_S = 4$, $N_D = 24$, $N_V = 12$ imply the fixed point

$$\text{SMRHN: } \tilde{G}^* = 3.56, \quad \tilde{\Lambda}^* = -5.35, \quad (3.24)$$

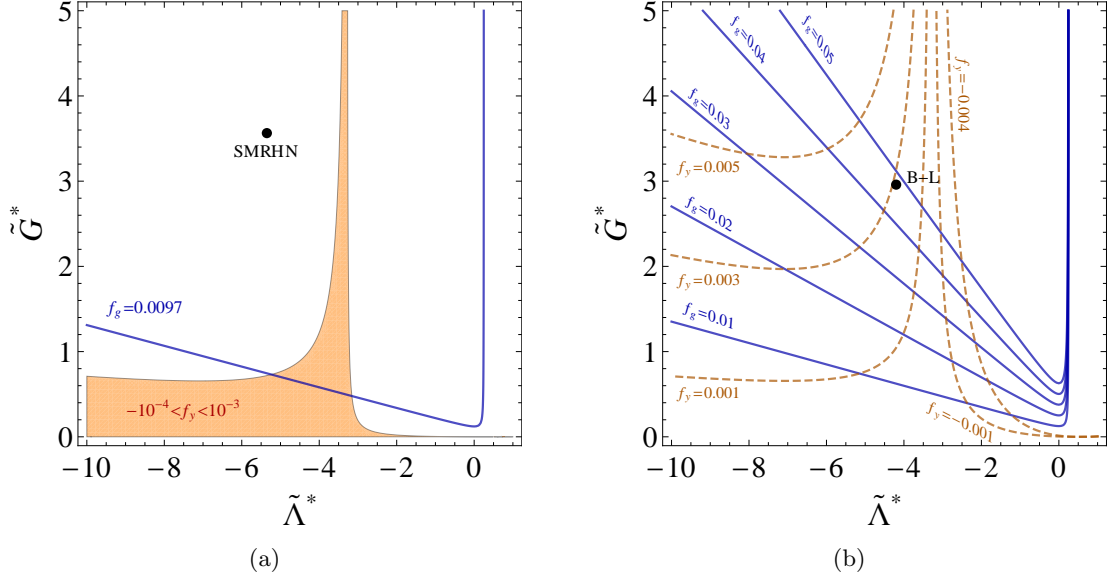


Figure 2: (a) The region of $(\tilde{\Lambda}^*, \tilde{G}^*)$ parameter space consistent with a small neutrino Yukawa coupling in the SMRHN. Blue solid line shows $f_g = 0.0097$, which is required for generating an irrelevant $g_Y^* \neq 0$. Orange region is consistent with the \overline{MS} value of the top mass. Black dot shows the outcome of a calculation with FRG techniques [47]. (b) The same in the $B-L$ model. All contours of f_g (solid blue) are consistent with a small neutrino Yukawa coupling. f_y contours (dashed brown) will be subject to constraints described in detail in Sec. 4. Black dot shows the outcome of a calculation with FRG techniques [47].

which is indicated as a black dot in Fig. 2(a). If Eq. (2.3) is taken at face value one gets $f_g = 0.046$, $f_y = 0.0050$. Even taking into account that the given explicit forms of Eqs. (2.3), (3.22), and (3.23) are all sensitive to the chosen action truncation and gauge [68], and that one cannot *a priori* exclude that, after all sources of theoretical uncertainty were accounted for, the final expression may well allow for the black dot to sit right inside the phenomenologically preferred region, it is nonetheless disappointing that in the SMRHN the dynamical generation of a small Yukawa coupling depends strongly on effects that are not currently under control.

Conversely, one can recast the above discussion in the framework of the gauged $B-L$ model. Now, $N_S = 6$, $N_D = 24$, $N_V = 13$ yield the fixed point

$$B-L: \quad \tilde{G}^* = 2.96, \quad \tilde{\Lambda}^* = -4.20, \quad (3.25)$$

which corresponds to $f_g = 0.047$, $f_y = 0.0028$, and is indicated as a black dot in Fig. 2(b). We draw in Fig. 2(b) as solid blue contours some sample values of f_g , which are *all* currently allowed by phenomenological constraints and give rise to different predictions for the $B-L$ gauge coupling and kinetic mixing. Brown dashed lines show the contours of selected values of f_y . As we shall see in Sec. 4, the question of which of those values can lead to a top-quark mass determination in agreement with observations depends on the size of f_g and

f_g	g_Y^*	Other Abelian	Dynamical Mechanism
0.0097	0.47 (irr.)	$g_X^* = g_\epsilon^* = 0$ (rel.)	yes
		$g_X^* = 0.44, g_\epsilon^* = -0.34$ (irr.)	no
$f_g > 0.0097$	0 (rel.)	$g_X^* = g_\epsilon^* = 0$ (rel.)	no
		$12g_X^{*2} + \frac{32}{3}g_X^*g_\epsilon^* + \frac{41}{6}g_\epsilon^{*2} - 16\pi^2 f_g = 0$ (irr.)	yes

Table 1: Trans-Planckian fixed points of the abelian gauge sector of the $B - L$ model, as a function of f_g . Fixed points can be either relevant (rel.), *i.e.* UV-attractive, or irrelevant (irr.), *i.e.* IR-attractive.

has to be addressed on a case-by-case basis. Nevertheless, it appears that the spectrum of possibilities for the eventual outcome of an FRG calculation opens up significantly in the $B - L$ model with respect to the SMRHN.

4 Boundary conditions of the $B - L$ model

4.1 Fixed points of the gauge-Yukawa system

We discuss in this section the trans-Planckian fixed points of the $B - L$ gauge-Yukawa RGE system, whose explicit form can be found in Appendix A. We limit our discussion to real fixed points consistent with the dynamical generation of an arbitrarily small Yukawa coupling for the neutrino. We reiterate that in the $B - L$ model this is a viable possibility for all values of $f_g \geq 0.0097$.

We summarize in Table 1 the fixed points of the abelian gauge sector corresponding to different f_g values. The first line features the case equivalent to the SMRHN: f_g adopts the specific value making g_Y^* irrelevant, while the other two gauge couplings are relevant and become free parameters of the theory. They can thus be adjusted to fit all existing constraints.

The second line shows the fixed point with three irrelevant interactive gauge couplings. In this case, however, the gauge-Yukawa system does not admit an irrelevant fixed point with $y_\nu^* = 0$ if y_t^* is required to be real.

Increasing the value of f_g allows one to find a relevant Gaussian solution $g_Y^* = 0$. However, no irrelevant fixed point with $y_\nu^* = 0$ can be identified when all three abelian gauge couplings correspond to relevant directions (line 3 of Table 1). Thus, the fixed points of the two abelian NP couplings g_X and g_ϵ must be irrelevant (line 4). It turns out that they are not independent, but instead belong to an ellipse, parameterized by f_g :

$$12g_X^{*2} + \frac{32}{3}g_X^*g_\epsilon^* + \frac{41}{6}g_\epsilon^{*2} - 16\pi^2 f_g = 0. \quad (4.1)$$

Let us focus on the set of fixed points (4.1). As the size of the ellipse is determined by f_g , a larger f_g (perhaps from the FRG) will result in larger values for the fixed points of the $B - L$ gauge coupling and kinetic mixing. Additionally, the full RGE system is subject to bounds from the Yukawa sector, which constrain the size of f_g on a case-by-case basis.

Let us recall that the Yukawa sector of the $B - L$ model consists of several couplings, for which we seek the following trans-Planckian irrelevant fixed points:

$$y_t^* \neq 0, \quad y_\nu^* = 0, \quad y_N^* = 0 \text{ or } y_N^* \neq 0. \quad (4.2)$$

Note that we assume $y_t^* \neq 0$ in Eq. (4.2). This is required to obtain a negative critical exponent for the neutrino Yukawa couplings, as can be inferred by plugging into Eqs. (3.9)-(3.12) the numerical coefficients corresponding to the RGEs of the $B - L$ model. The fixed points of the three sterile neutrino Yukawa couplings are assumed to be degenerate, $y_N^{ii*} = y_N^*$, in both the Gaussian and interactive case. Similarly $y_\nu^{ii*} = y_\nu^*$. The choice $y_N^* = 0$ would correspond to the absence of the Majorana mass term in Eq. (3.17), thus leading to purely Dirac light neutrinos.

The trans-Planckian fixed-point value of the top quark Yukawa coupling is directly determined by f_y as

$$y_t^* = \sqrt{\frac{8g_X^{*2} + 20g_X^*g_\epsilon^* + 17g_\epsilon^{*2} + 192\pi^2 f_y}{54}}. \quad (4.3)$$

We impose $0.255 \leq y_t^* \leq 0.325$. If we decouple gravity sharply at $M_{\text{Pl}} = 10^{19}$ GeV the chosen range leads to the low-scale Yukawa coupling being consistent, within a few GeV uncertainty, with the \overline{MS} top quark mass. Such constraint loosely links the range of f_y to the value of f_g , which is what determines the size of g_X^* and g_ϵ^* in Eq. (4.3). One should thus take notice that in the $B - L$ model f_g and f_y are not entirely independent from one another, as they are correlated by the low-scale phenomenology.

We impose several other conditions on the Yukawa sector:

- y_t^* has to be real, *i.e.*, $17g_\epsilon^{*2} + 20g_X^*g_\epsilon^* + 8g_X^{*2} + 192\pi^2 f_y > 0$. This also guarantees that the top Yukawa coupling is irrelevant, $\theta_t < 0$.
- $y_\nu^* = 0$ has to be irrelevant, *i.e.*, $\theta_\nu < 0$.
- if $y_N^* \neq 0$, it has to be real, *i.e.*, $3g_X^{*2} + 8\pi^2 f_y > 0$. This also guarantees that y_N is irrelevant, $\theta_N < 0$.
- if $y_N^* = 0$, it has to be irrelevant, *i.e.*, $\theta_N = 3g_X^{*2} + 8\pi^2 f_y < 0$.

We show in Fig. 3 the regions of the (g_X^*, g_ϵ^*) plane subject to the constraints listed above. The color scheme is described in detail in the caption. We select (a) $f_y = 0.0005$, (b) $f_y = -0.005$, (c) $f_y = -0.0015$, and (d) $f_y = -0.004$. In all panels, black dots mark the position of selected benchmark points. We report their characteristic features in Table 2.

The last three columns of Table 2 show the predicted values of irrelevant couplings g_X , g_ϵ , and y_N at three sub-Planckian scales of interest, 10^5 GeV, 10^7 GeV, and 10^9 GeV. Those are our chosen reference scales for the analysis of gravitational wave signatures in Sec. 5.³

³Note that low-scale predictions originating from the trans-Planckian fixed-point analysis are derived under the assumption that the RGEs are not altered by large couplings below the Planck scale. Therefore, any additional low-scale interaction ought to be feeble. This is a commonly adopted approach in phenomenological studies with AS, as was discussed in Refs. [72, 81].

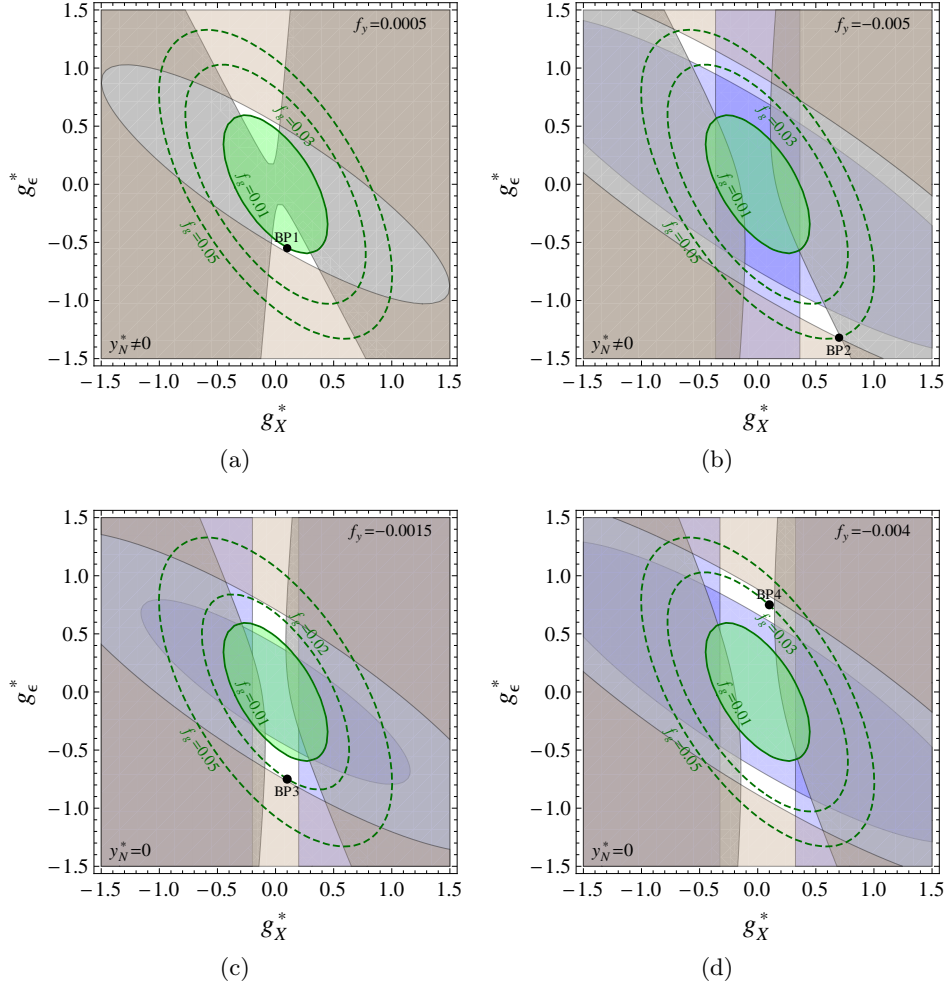


Figure 3: (a) Dashed green ellipses trace the fixed-point solutions of Eq. (4.1) for different values of f_g . The inner green region, $f_g < 0.0097$, is excluded by the low-scale determination of the hypercharge gauge coupling. For $f_y = 0.0005$, brown shading excludes the parameter space which does not allow the matching of the correct value of the top mass at the low scale, and the gray region indicates the parameter space in which critical exponent $\theta_\nu > 0$ at $y_\nu^* = 0$, *i.e.*, there is no dynamical generation of a small Yukawa coupling. The white region is phenomenologically viable and we indicate with a black dot benchmark point BP1 (see also Table 2). (b) Same as (a), but $f_y = -0.005$. The elliptical and vertical blue shaded regions indicate, respectively, the values of the gauge couplings for which y_t^* and y_N^* are imaginary. Black dot indicates benchmark point BP2. (c) Same as (a), but $f_y = -0.0015$. The elliptical and vertical blue shaded regions indicate, respectively, the values of the gauge couplings for which y_t^* is imaginary and y_N is relevant. Black dot indicates benchmark point BP3. (d) Same as in (c), but $f_y = -0.004$. Black dot indicates benchmark point BP4.

	f_g	f_y	g_X^*	g_ϵ^*	y_N^*	$g_X (10^{5,7,9} \text{ GeV})$	$g_\epsilon (10^{5,7,9} \text{ GeV})$	$y_N (10^{5,7,9} \text{ GeV})$
BP1	0.01	0.0005	0.10	-0.55	0.12	0.29, 0.29, 0.30	-0.26, -0.27, -0.28	0.16, 0.16, 0.16
BP2	0.05	-0.005	0.70	-1.32	0.47	0.40, 0.41, 0.44	-0.52, -0.56, -0.61	0.42, 0.44, 0.45
BP3	0.02	-0.0015	0.10	-0.75	0.0	0.12, 0.12, 0.12	-0.33, -0.35, -0.37	0.0
BP4	0.03	-0.004	0.10	0.75	0.0	0.09, 0.09, 0.09	0.23, 0.25, 0.28	0.0

Table 2: The values of f_g and f_y , trans-Planckian fixed points of the irrelevant couplings (indicated with an asterisk), and predicted values of those couplings at three low scales of reference for the four benchmark points selected in this study. All four points admit irrelevant $y_\nu^* = 0$.

BP1 and BP2 feature $y_N^* \neq 0$, which is of order 1 in size. Equation (3.17) implies in this case that the Majorana mass scale is $M_N = \sqrt{2}y_N v_S$. It is a canonically relevant parameter of the theory and can thus be chosen anywhere, as long as it is in agreement with phenomenological constraints on the scalar potential. Note that the see-saw mechanism can be here invoked to give mass to the active neutrinos, $m_\nu \sim y_\nu^2 v_H^2 / (\sqrt{2}M_N)$. The theory is consistent with AS whatever the Majorana mass scale is, since the correct size of the neutrino Yukawa coupling can be generated dynamically in the trans-Planckian flow.

On the other hand, BP3 and BP4 in Table 2 feature $y_N^* = 0$ along irrelevant directions, similarly to y_ν^* . These cases allow for the interesting possibility that the sterile-neutrino Yukawa coupling sits tight at the irrelevant Gaussian fixed point $y_N^* = 0$. The Majorana mass is never generated, and its absence is protected along the entire RG flow by quantum scale invariance. The theory thus supports Dirac neutrinos with mass $m_\nu \sim y_\nu v_H / \sqrt{2}$, where the required minuscule Yukawa coupling is generated dynamically.

In alternative, the theory might originate from a UV-attractive y_N fixed point, and dynamically flow towards the IR-attractive one, thus generating – besides an arbitrarily small y_ν – also an arbitrarily small y_N . This case supports the existence of a Majorana mass, but the latter may be naturally decoupled from the size of v_S and the constraints on the scalar potential. Thus, BP3 and BP4 may additionally provide a natural framework for accommodating the phenomenologically interesting possibility of pseudo-Dirac neutrinos [14].

4.2 Scalar potential

The tree-level scalar potential of the gauged $B - L$ model is given by

$$V(H, S) = m_H^2 H^\dagger H + m_S^2 S^\dagger S + \lambda_1 (H^\dagger H)^2 + \lambda_2 (S^\dagger S)^2 + \lambda_3 (H^\dagger H) (S^\dagger S), \quad (4.4)$$

where H is the SM-like Higgs $SU(2)_L$ doublet, which is neutral under $U(1)_{B-L}$, and S is a complex scalar SM singlet, charged under $U(1)_{B-L}$ with $Q_S = 2$. The spontaneous breaking of $U(1)_{B-L}$ generates the mass of the abelian Z' gauge boson, which is approximately proportional to the vev along the S direction: $m_{Z'} \approx 2 g_X v_S$.

The benchmark points in Table 2 are all characterized by large kinetic mixing,

$$\epsilon = \frac{g_\epsilon}{\sqrt{g_Y^2 + g_\epsilon^2}} \approx 0.5 - 0.8. \quad (4.5)$$

As a direct consequence, $m_{Z'}$ is bounded from below by direct LHC constraints on high-mass dilepton resonance searches. The most recent measurements by ATLAS [92] and CMS [93], based on the 140/fb data set in proton–proton collisions at the centre-of-mass energy of $\sqrt{s} = 13$ TeV was numerically recast to the $(m_{Z'}, \epsilon)$ plane in Fig. 3 of Ref. [81]. Since in our case the Z' gauge boson couples directly to the quarks of the first two generations, the actual lower bound on the Z' mass is stronger than for a dark gauge boson coupling to the quarks only through the kinetic mixing. For the four benchmark points in Table 2 one finds $m_{Z'} \gtrsim 6$ TeV, which implies the following bounds on the vev of S :

$$\text{BP1: } v_S \gtrsim 10 \text{ TeV} \quad (4.6)$$

$$\text{BP2: } v_S \gtrsim 7.5 \text{ TeV} \quad (4.7)$$

$$\text{BP3: } v_S \gtrsim 25 \text{ TeV} \quad (4.8)$$

$$\text{BP4: } v_S \gtrsim 33 \text{ TeV}. \quad (4.9)$$

We have checked that the LHC direct measurements are currently more constraining than the bounds from the ρ_0 precision parameter [94], which require, for the same kinetic mixing, $m_{Z'} \gtrsim 2$ TeV.

Since $v_S \gg v_H = 246$ GeV, the two directions of the scalar potential effectively decouple. The vev v_S may arise from the presence of a large mass m_S^2 in Eq. (4.4). However, in this work we rather decide to investigate the well-known possibility that the scalar potential of the $B - L$ model develop its vevs from dimensional transmutation [95–99], through the usual Coleman-Weinberg mechanism. In particular, we next discuss whether the possibility of developing a radiatively generated minimum is consistent with the benchmark points in Table 2 and with AS in general.

Let us define $\phi \equiv \sqrt{2} \text{Re}(S)$, and project the potential to the ϕ direction. The corresponding, RGE-improved Coleman-Weinberg potential in the $B - L$ model reads (cf. Appendix B)

$$V(\phi) = \frac{1}{2} m_S^2(t) \phi^2 + \frac{1}{4} \lambda_2(t) \phi^4 + \frac{1}{128 \pi^2} [20 \lambda_2^2(t) + 96 g_X^4(t) - 48 y_N^4(t)] \phi^4 \left(-\frac{25}{6} + \ln \frac{\phi^2}{\mu^2} \right), \quad (4.10)$$

where $t = \ln \mu$ is the renormalization scale. The potential can develop a minimum due to a large finite 1-loop contribution. If at the scale μ one finds

$$\lambda_2 \approx \frac{1}{55} \left(12 \pi^2 - 2 \sqrt{-3630 g_X^4 + 1815 y_N^4 + 36 \pi^4 + 330 \pi^2 m_S^2 / \mu^2} \right), \quad (4.11)$$

the minimum resides at $v_S \approx \mu$.

Constraints apply from EWSB,

$$M_h^2 = -2m_H^2 - \lambda_3 v_S^2 \quad (4.12)$$

$$v_H^2 = \frac{-2m_H^2 - \lambda_3 v_S^2}{2\lambda_1}, \quad (4.13)$$

where M_h is the Higgs mass and v_H is the SM Higgs doublet vev. For $m_H^2, v_H^2 \ll v_S^2$, these typically require $|\lambda_3(v_S)| \ll \lambda_1(v_S)$.

It is interesting to investigate whether the Coleman-Weinberg construction is consistent with boundary conditions originating from trans-Planckian AS. A complementary analysis of the $B - L$ scalar potential in AS can be found, *e.g.*, in Ref. [83].

Let us define the dimensionless running parameters $\tilde{m}_H^2 = m_H^2/\mu^2$ and $\tilde{m}_S^2 = m_S^2/\mu^2$. The RGEs of the scalar potential are modified in the trans-Planckian regime with a “correction” due to the gravity fixed points, in analogy to Eqs. (2.1) and (2.2). Following several studies in the literature [100–102] one writes

$$\frac{d\lambda_1}{dt} = 4\eta_1\lambda_1 + \beta_{\lambda_1,\text{add}}(g_i, y_j, \lambda_k) - f_\lambda\lambda_1 + \beta_{\lambda_1,\text{grav}} \quad (4.14)$$

$$\frac{d\lambda_2}{dt} = 4\eta_2\lambda_2 + \beta_{\lambda_2,\text{add}}(g_i, y_j, \lambda_k) - f_\lambda\lambda_2 + \beta_{\lambda_2,\text{grav}} \quad (4.15)$$

$$\frac{d\lambda_3}{dt} = 2(\eta_1 + \eta_2)\lambda_3 + \beta_{\lambda_3,\text{add}}(g_i, y_j, \lambda_k) - f_\lambda\lambda_3 + \beta_{\lambda_3,\text{grav}} \quad (4.16)$$

$$\frac{d\tilde{m}_H^2}{dt} = (-2 + 2\eta_1)\tilde{m}_H^2 + \beta_{\tilde{m}_H^2,\text{add}}(\tilde{m}_H^2, \tilde{m}_S^2) - f_\lambda\tilde{m}_H^2 \quad (4.17)$$

$$\frac{d\tilde{m}_S^2}{dt} = (-2 + 2\eta_2)\tilde{m}_S^2 + \beta_{\tilde{m}_S^2,\text{add}}(\tilde{m}_H^2, \tilde{m}_S^2) - f_\lambda\tilde{m}_S^2, \quad (4.18)$$

where the matter anomalous dimensions η_1 and η_2 are given in Eqs. (A.10), (A.11) of Appendix A. The terms with an “add” subscript parameterize additive contributions to the matter beta functions not included in the anomalous dimensions, which are given explicitly in Eqs. (A.12)–(A.16). f_λ is the universal multiplicative correction analogous to f_g and f_y , which typically depends on the fixed points of the gravitational action. Finally, the terms with a “grav” subscript parameterize additive contributions potentially arising from non-minimal direct couplings of the scalar potential to gravitational operators, see, *e.g.*, the truncation introduced in Ref. [73].

One may categorize the outcome of the eventual FRG calculation of f_λ in three broad classes inducing different qualitative behavior:

Case A. $f_\lambda \ll -2$. Under this condition Eqs. (4.17) and (4.18) admit the Gaussian fixed point $\tilde{m}_H^{2*} = 0$, $\tilde{m}_S^{2*} = 0$, fully irrelevant. The potential of Eq. (4.4) becomes thus scale-invariant and it remains so at all scales, protected by quantum scale symmetry. It was shown in Refs. [100–102] that $f_\lambda \ll -2$ may emerge in FRG calculation of the Higgs potential and Einstein-Hilbert truncation of the gravitational action, for certain values of the running Planck mass.

In the context of the $B - L$ model with Coleman-Weinberg potential, conformal symmetry makes the model very predictive. After solving Eqs. (4.12) and (4.13) for λ_1, λ_3

with $M_h = 125 \text{ GeV}$, $v_H = 246 \text{ GeV}$, one derives the values of the couplings at the scale of reference v_S . For example, at $v_S = 10^5 \text{ GeV}$,

$$\lambda_1(10^5 \text{ GeV}) \approx 0.05, \quad \lambda_3(10^5 \text{ GeV}) \approx -1.5 \times 10^{-6}. \quad (4.19)$$

On the other hand, one can solve Eqs. (4.14)-(4.16) to obtain the boundary conditions at the Planck scale in terms of the fixed points of Table 2. In the absence of non-minimal gravitational (“grav”) contributions one finds

$$\begin{aligned} \lambda_1^* &\approx -\frac{\beta_{\lambda_1, \text{add}}(g_i^*, y_j^*, \lambda_k^*)}{|f_\lambda|} \approx -\frac{\frac{3}{8}g_\epsilon^{*4} - 6y_t^{*4}}{16\pi^2|f_\lambda|} \\ \lambda_2^* &\approx -\frac{\beta_{\lambda_2, \text{add}}(g_i^*, y_j^*, \lambda_k^*)}{|f_\lambda|} \approx -\frac{96g_X^{*4} - 48y_N^{*4}}{16\pi^2|f_\lambda|} \\ \lambda_3^* &\approx -\frac{\beta_{\lambda_3, \text{add}}(g_i^*, y_j^*, \lambda_k^*)}{|f_\lambda|} \approx -\frac{12g_X^{*2}g_\epsilon^{*2}}{16\pi^2|f_\lambda|}, \end{aligned} \quad (4.20)$$

all of them along irrelevant directions. Since the fixed points (4.20) are suppressed by large $|f_\lambda|$, λ_1^* , λ_2^* , and λ_3^* are predicted to be extremely close to zero at the Planck scale and, as a consequence, the boundary conditions (4.20) are not consistent with Eqs. (4.19) after following the RG flow of the quartic couplings to IR energies.

Even more damning for this case is perhaps the fact that following the flow of λ_2 from the Planck scale to the low energy one obtains large negative values (*e.g.*, $\lambda_2 = -0.56$ at $v_S = 10^5 \text{ GeV}$), which end up destabilizing the scalar potential from below in the S direction (see also Ref. [83], where the same conclusion was reached). These considerations make us conclude that Case A may be phenomenologically viable only in the presence of some specific truncations of the gravitational action [73]. In particular, a substantial $\beta_{\lambda_2, \text{grav}} < 0$ at the fixed point will be required to match the low-energy phenomenology, implying, possibly, some fine tuning.

Case B. $-2 \lesssim f_\lambda < 0$. An eventual outcome of the FRG calculation within this range would imply that the fixed point at $\tilde{m}_H^2 = 0$, $\tilde{m}_S^2 = 0$ is fully relevant, while the fixed points (4.20) of the quartic couplings are irrelevant. As such, the latter remain predictions of the theory at all scales, whereas the former are effectively free parameters. At the low scale, m_H^2 can be determined by solving Eq. (4.12) once λ_3 is known. However, no realistic value of $f_\lambda < 0$ can generate a fixed-point value $\lambda_2^* > 0$ large enough to avoid the destabilization of the potential at low energies. As we concluded in Case A, in Case B as well one has to rely on the non-minimal contributions to the beta function parameterized by $\beta_{\lambda_2, \text{grav}}$.

Case C. $f_\lambda \gg 0$. In this case the fixed points of the scalar potential are relevant. Masses and quartic couplings cannot be predicted from UV considerations, as any adopted value is eventually consistent with AS. It was shown in Ref. [101] that $f_\lambda > 0$ cannot be an outcome of the FRG calculation with the action comprising the SM Higgs potential and gravity in the Einstein-Hilbert truncation, independently of the fixed-point value of the gravitational parameters and of the choice of regulator.

On the other hand, it was recently shown in Ref. [71] that the situation may be different if one keeps track in the FRG calculation of several higher-order operators arising from a Taylor expansion of the SM Higgs potential. One can then observe the emergence of a second relevant direction at the Gaussian fixed point, in addition to the one typically associated with $m_H^{2*} = 0$. This additional relevant direction, which remains hidden in calculation performed in a $\mathcal{O}(H^4)$ truncation, is indeed welcome as it allows a phenomenologically viable connection between the UV fixed point and the physical SM at low energies. For the purposes of this paper, which is phenomenological in spirit, we assume that a similar behavior can be extended to the S direction of the $B - L$ scalar potential, effectively allowing us to consider $f_\lambda \gg 0$ in Eqs. (4.14)-(4.16) and connecting the asymptotically safe fixed point in the deep UV to any desired Planck-scale boundary condition for the quartic couplings.

5 Gravitational waves

It has long been known that a GW signal from the $B - L$ FOPT can be strong enough to allow detection in new-generation interferometers [103–108]. It is therefore enticing to investigate predictions for GWs associated with the boundary conditions from trans-Planckian AS discussed in Sec. 4.

In the presence of a hot plasma in the early Universe, the effective scalar potential receives thermal corrections [109, 110], which generate a thermal barrier between the false ($\phi = 0$) and true ($\phi = v_S$) $B - L$ vacua (cf. Appendix B). Tunneling from the former to the latter can then proceed through bubble nucleation [111, 112], leading to the generation of GWs.

The GW physics is governed by several parameters that mainly depend on the shape of the effective thermal potential and on the bubbles' profile. These are the latent heat α , the nucleation speed β , and the reheating temperature T_{rh} . We refer the reader to Appendix C for a brief review of the physics of FOPTs. The present-day GW signal is then characterized by the peak amplitude $\Omega^{\text{peak}}(\alpha, \beta, T_{\text{rh}})$ and the peak frequency $f^{\text{peak}}(\alpha, \beta, T_{\text{rh}})$,

$$h^2 \Omega_{\text{GW}}(f) = h^2 \Omega^{\text{peak}} \times \mathcal{F}(f/f^{\text{peak}}), \quad (5.1)$$

where $h = H_0/(100 \text{ km/s/Mpc})$ is the present-day dimensionless Hubble parameter and \mathcal{F} is a function of the frequency f . The explicit forms of the GW signal amplitudes are collected in Eqs. (C.10)-(C.12) of Appendix C.

We calculate the GW spectra for the benchmark points listed in Table 2. The tree-level scalar mass m_S^2 plays an important role in the phenomenological prediction. In Case A of Sec. 4.2 we considered $f_\lambda \ll -2$, so that $m_S^2 = 0$ is protected by quantum scale symmetry. Scale invariance is typically associated with strong supercooling, and may give rise to large GW signals [113–117]. The presence of Yukawa couplings $y_N \neq 0$ is another key factor determining the properties of the FOPT. The height of the thermal barrier is directly proportional to y_N – cf. Eq. (B.6) and Eq. (B.9) in Appendix B – forcing the nucleation and percolation temperature to be lower than with $y_N = 0$ and therefore enhancing the impact of supercooling. This effect is particularly prominent for BP2, where we find that

$T_p < 0.1$ GeV, independently of the chosen value of v_S . At $T \approx 0.1$ GeV the QCD phase transition takes place, a case that we do not analyze in this study.

We observe the same behavior in BP1 at $v_S = 10^9$ GeV. Conversely, for BP1 at $v_S = 10^5, 10^7$ GeV, the non-zero value of y_N sets the nucleation/percolation temperature at several GeV. At the same time, $y_N \neq 0$ makes the Coleman-Weinberg minimum shallower, so that the probability of tunneling at a given temperature is reduced. As a result, the nucleation termination condition, Eq. (C.5) in Appendix C, is not satisfied. Those effects combined lead us to the conclusion that no GW signal can be observed for BP1 and BP2 with $m_S^2 = 0$.

BP3 and BP4 are characterized by relatively small values of the $B - L$ coupling. The Coleman-Weinberg minimum is thus rather shallow, indicating low decay rate of the false vacuum, $S_3(T)/T \gg 100$. As a result, there is no FOPT in BP3 and BP4 when $m_S^2 = 0$ for all chosen values of v_S .

Meanwhile, we discussed in Sec. 4.2 that the purely conformal case, $m_S^2 = 0$, may be in strong tension with the requirement of a stable (bounded from below) scalar potential at the chosen scales v_S , unless one considers non-minimal terms in the matter-gravity action, which are likely to involve some fine tuning. A more natural possibility in the quantum gravity setup is thus that the mass terms in Eq. (4.4) remain relevant parameters, in agreement with their canonical scaling, a situation described in Case B and Case C of Sec. 4.2. No quantum scale symmetry can in those cases prevent the presence of tree-level masses in the Lagrangian. On the other hand, since $|\lambda_3| \ll 1$, the mass parameters appear, to a good approximation, multiplicatively in their respective RGEs – Eqs. (4.17) and (4.18) – and are thus technically natural. As a consequence, they can take any desired value. We consider here the situation where $m_S^2 < 0$ is small enough not to interfere with the generation of a thermal barrier – the transition is still first order – but large enough to enhance the decay rate of the false vacuum given in Eq. (C.1), thus triggering the phase transition at nucleation (and percolation) temperature larger than it would be required in the conformal case.

We present in Fig. 4 the expected GW signal at $v_S = 10^5$ GeV for the four benchmark points in Table 2 given two selected values of the mass: $\sqrt{|m_S^2|} = 1$ GeV (yellow) and $\sqrt{|m_S^2|} = 1$ TeV (red). The signal is confronted with integrated sensitivity curves for the Big-Bang Observer (BBO) [118, 119], Cosmic Explorer (CE) [120], Deci-Hertz Interferometer Gravitational-Wave Observatory (DECIGO) [121, 122], Einstein Telescope (ET) [123, 124], Laser Interferometer Gravitational-Wave Observatory (LIGO) [125–127] and Laser Interferometer Space Antenna (LISA) [128, 129], which are shown as dotted curves. Gray region in the upper part of the plot indicates the current exclusion bound by the LIGO-VIRGO O2 run [130, 131].

Benchmark point BP1 is shown in panel (a) and BP2 in panel (b). Despite obtaining in the two cases quite different predictions from the fixed-point analysis, we observe similar GW amplitudes and frequencies. This is because the phase transitions are triggered by the mass term, so that they feature, given equivalent $m_S^2 < 0$, a similar, relatively fast nucleation speed β . Analogous behavior is observed for BP3 in panel (c) and BP4 in

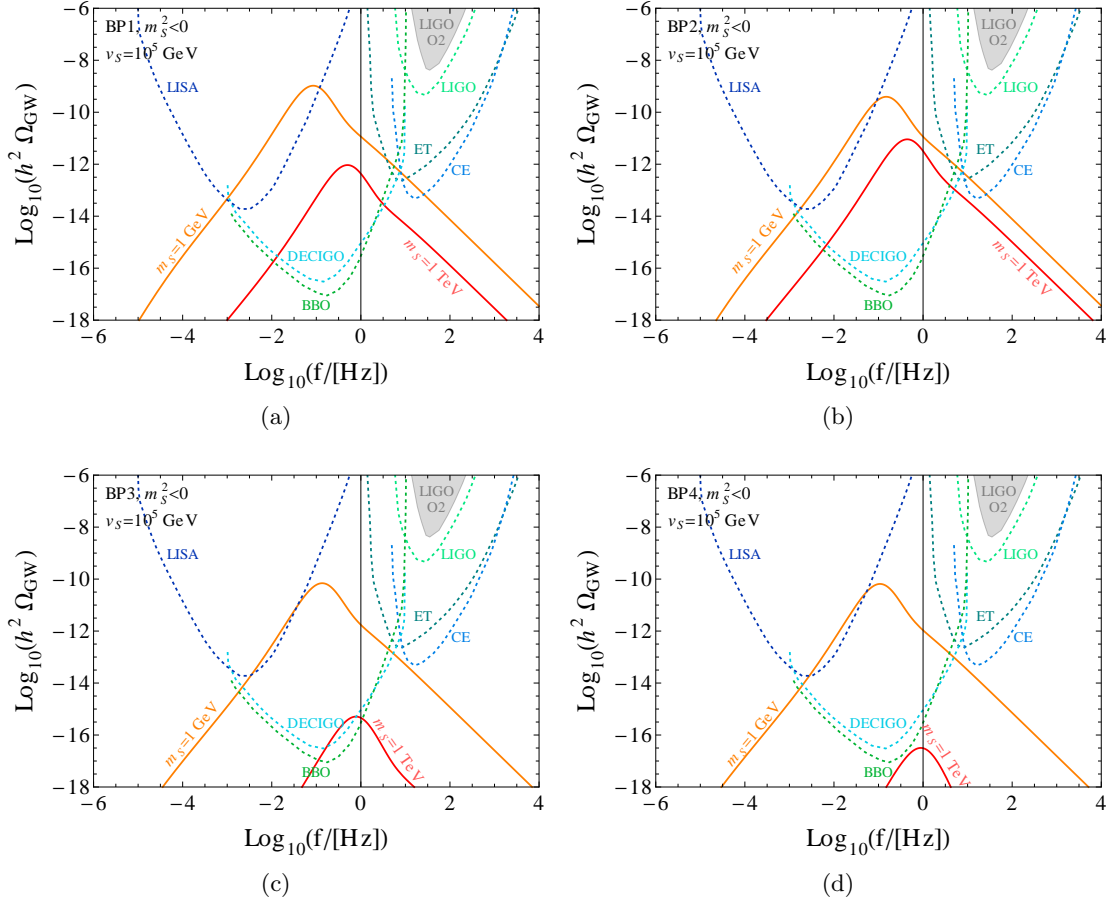


Figure 4: Gravitational-wave spectra of the benchmark points listed in Table 2, for two selected values of the scalar mass parameter $m_S \equiv \sqrt{|m_S^2|}$ (solid lines). The scalar vev is set at $v_S = 10^5$ GeV. Also shown are the sensitivity curves for various GW interferometers (dotted lines).

panel (d), with the biggest difference with respect to BP1 and BP2 being that the signal amplitude and frequency show greater sensitivity to the m_S^2 spread. This is due to the much lesser depth of the minimum in BP3 and BP4, which enhances the impact of a finite m_S^2 on the bounce action. All in all, we observe strong similarities of signatures in the four cases. We are thus forced to conclude that different fixed points cannot be distinguished with a detection of GWs from FOPTs. Equally bleak are the prospects of distinguishing the Majorana vs. Dirac nature of the neutrino with this method, since the fixed points with $y_N^* \neq 0$ and those with $y_N^* = 0$ show very similar spectra, shaped in all cases by the m_S^2 relevant parameter.⁴

We finally show in Fig. 5 the GW signal of BP1 with $\sqrt{|m_S^2|} = 1$ GeV for all the v_S values given in Table 2. As is well known, larger vev induces a signal at larger frequency.

⁴The situation may be more optimistic if the dynamical mechanism for the generation of neutrino masses relies on a UV completion that gives rise to topological defects [132].

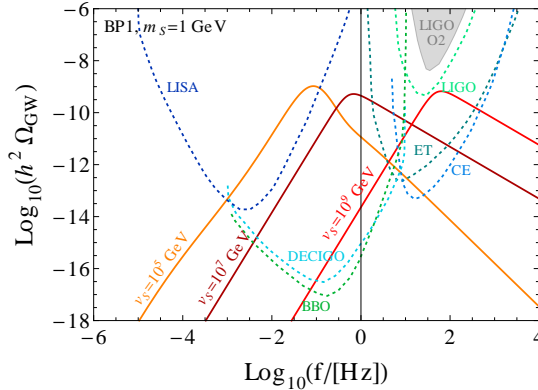


Figure 5: Gravitational-wave spectra of benchmark point BP1, for increasing values of the scalar vev v_S (solid lines). The scalar mass parameter is set at $m_S \equiv \sqrt{|m_S^2|} = 1$ GeV. Also shown are the sensitivity curves for various GW interferometers (dotted lines).

More interestingly, one can see that while at $v_S = 10^5$ GeV (orange) the main source of GW is sound waves and turbulence of the plasma, for larger values (brown and red) the main source is bubble collisions, which flatten the signal at higher frequencies. This is because, as the critical temperature increases with the vev, the percolation temperature remains set at approximately the same value, determined by the size of m_S^2 . The overall effect is thus to increase the amount of supercooling with larger vevs.

6 Conclusions

In this paper, we have revisited the dynamical generation of an arbitrarily small neutrino Yukawa coupling based on the existence of Gaussian IR-attractive fixed points of the trans-Planckian RG flow, which was investigated first in Refs. [10, 11]. While in the original studies the low-energy theory that is completed in the UV with boundary conditions consistent with asymptotically safe quantum gravity was the SM with three right-handed neutrinos (SMRHN), in this work we have focused on the well-known gauged $B - L$ model.

The $B - L$ model offers several advantages with respect to the SMRHN. Some are well established – like requiring the existence of right-handed neutrino spinor fields based on the cancellation of gauge anomalies and the reliance on gauge rather than global or accidental symmetries – others apply more directly to the realm of trans-Planckian AS and the quantum-gravity nature of the UV completion.

On the one hand, we have shown that the $B - L$ model may justify a richer phenomenology in the context of neutrino mass-generation, since it seems to be able to accommodate quite naturally each and every feature that neutrinos may eventually show experimentally. Assuming in fact that there exists an IR-attractive fixed point at $y_\nu^* = 0$, trajectories of the RG flow originating from an irrelevant $y_N^* = 0$ will lead to purely Dirac neutrinos at the low scale; trajectories originating from a different, relevant y_N^* , whose trans-Planckian flow conjoins to the IR-attractive $y_N^* = 0$, may lead to pseudo-Dirac neutrinos; trajectories originating in an irrelevant $y_N^* \neq 0$ will lead straightforwardly to Majorana neutrinos, and

so on. The see-saw scale too, being a canonically relevant parameter of the Lagrangian, can freely assume any desired value.

On the other hand, we have shown that this rich phenomenology may be found to be in better agreement with calculations of the quantum gravity UV completion, which are likely to be based on FRG techniques. In fact, in the SMRHN a very specific, potentially fine-tuned value of the gravity contribution f_g is required, lest we risk failing to reproduce the measured low-scale hypercharge coupling. This is not the case in the $B - L$ model, as the dynamical role played by the irrelevant g_Y fixed point in the SMRHN is here enacted through the fixed points of the $B - L$ gauge coupling and kinetic mixing. This gives us the ability to untie the results of the first-principle calculation in quantum gravity – which are marred by significant theoretical uncertainties – from the precise measurement of a well-known quantity at the low scale, opening up the spectrum of observable possibilities.

Among the several interesting signatures of the model, we investigated in detail the generation of gravitational waves from FOPTs. For our four different benchmark points we found that, while it will be easy to observe a clear signal in future interferometers, it will prove extremely more challenging to be able to discern different fixed points – their gauge and Yukawa coupling values and, more importantly, the Majorana vs. Dirac nature of the neutrino – from one another. This is because an explicit mass term in the effective scalar potential is necessary to trigger the $B - L$ phase transition. While this is a welcome feature for the theoretical consistency of the model – scalar masses are relevant parameters within the trans-Planckian UV completion so that conformal symmetry is not a property enforced by RG running – it also makes the GW spectrum extremely sensitive to parameters that cannot, by their own nature, be predicted from UV considerations. Even if a GW signal were to be detected, additional observations in complementary experimental venues – for example, the detection of new spin-0 and spin-1 resonances in multilepton searches at future high-energy colliders – will be required to extract unequivocally the shape of the potential and uncover the UV nature of these fixed points.

ACKNOWLEDGMENTS

We would like to thank Anish Ghoshal for many discussions and Wojciech Kotlarski for help with PyR@TE. AC and EMS are supported in part by the National Science Centre (Poland) under the research Grant No. 2020/38/E/ST2/00126. KK is supported in part by the National Science Centre (Poland) under the research Grant No. 2017/26/E/ST2/00470. The use of the CIS computer cluster at the National Centre for Nuclear Research in Warsaw is gratefully acknowledged.

A Renormalization group equations

In this appendix we present the RGEs of the gauged $B - L$ model, which we derive using PyR@TE 3 [133, 134]. Capital letters indicate a coupling matrix in flavor space. We work

at one loop, so that the trans-Planckian RGE of a generic gauge or Yukawa coupling c_i takes the form

$$\frac{dc_i}{dt} = \frac{1}{16\pi^2} \beta^{(1)}(c_i) - f_c c_i, \quad (\text{A.1})$$

where $f_c = f_g$ for all gauge couplings and $f_c = f_y$ for all Yukawa couplings.

Gauge couplings

$$\beta^{(1)}(g_Y) = \frac{41}{6} g_Y^3 \quad (\text{A.2})$$

$$\beta^{(1)}(g_\epsilon) = \frac{32}{3} g_Y^2 g_X + \frac{32}{3} g_X g_\epsilon^2 + \frac{41}{3} g_Y^2 g_\epsilon + 12 g_X^2 g_\epsilon + \frac{41}{6} g_\epsilon^3 \quad (\text{A.3})$$

$$\beta^{(1)}(g_X) = 12 g_X^3 + \frac{41}{6} g_X g_\epsilon^2 + \frac{32}{3} g_X^2 g_\epsilon \quad (\text{A.4})$$

$$\beta^{(1)}(g_2) = -\frac{19}{6} g_2^3 \quad (\text{A.5})$$

$$\beta^{(1)}(g_3) = -7 g_3^3. \quad (\text{A.6})$$

Yukawa couplings

$$\begin{aligned} \beta^{(1)}(Y_u) = & \frac{3}{2} Y_u Y_u^\dagger Y_u + 3 \text{Tr} \left(Y_u^\dagger Y_u \right) Y_u + \text{Tr} \left(Y_\nu^\dagger Y_\nu \right) Y_u \\ & - \frac{17}{12} g_Y^2 Y_u - \frac{2}{3} g_X^2 Y_u - \frac{5}{3} g_X g_\epsilon Y_u - \frac{17}{12} g_\epsilon^2 Y_u - \frac{9}{4} g_2^2 Y_u - 8 g_3^2 Y_u \end{aligned} \quad (\text{A.7})$$

$$\begin{aligned} \beta^{(1)}(Y_\nu) = & \frac{3}{2} Y_\nu Y_\nu^\dagger Y_\nu + 2 Y_\nu Y_N^* Y_N + 3 \text{Tr} \left(Y_u^\dagger Y_u \right) Y_\nu + \text{Tr} \left(Y_\nu^\dagger Y_\nu \right) Y_\nu \\ & - \frac{3}{4} g_Y^2 Y_\nu - 6 g_X^2 Y_\nu - 3 g_X g_\epsilon Y_\nu - \frac{3}{4} g_\epsilon^2 Y_\nu - \frac{9}{4} g_2^2 Y_\nu \end{aligned} \quad (\text{A.8})$$

$$\beta^{(1)}(Y_N) = Y_\nu^T Y_\nu^* Y_N + Y_N Y_\nu^\dagger Y_\nu + 4 Y_N Y_N^* Y_N + 2 \text{Tr} (Y_N^* Y_N) Y_N - 6 g_X^2 Y_N. \quad (\text{A.9})$$

Anomalous dimensions and additive terms of the scalar potential

$$\eta_1 = \frac{1}{16\pi^2} \left[-\frac{3}{4} g_Y^2 - \frac{3}{4} g_\epsilon^2 - \frac{9}{4} g_2^2 + 3 \text{Tr} \left(Y_u^\dagger Y_u \right) + \text{Tr} \left(Y_\nu^\dagger Y_\nu \right) \right] \quad (\text{A.10})$$

$$\eta_2 = \frac{1}{16\pi^2} \left[-12 g_X^2 + 2 \text{Tr} (Y_N^* Y_N) \right] \quad (\text{A.11})$$

$$\begin{aligned} \beta_{\lambda_1, \text{add}}(g_i, y_j, \lambda_k) = & \frac{1}{16\pi^2} \left[24 \lambda_1^2 + \lambda_3^2 + \frac{3}{8} g_Y^4 + \frac{3}{4} g_Y^2 g_\epsilon^2 + \frac{3}{8} g_\epsilon^4 + \frac{3}{4} g_Y^2 g_2^2 + \frac{3}{4} g_2^2 g_\epsilon^2 + \frac{9}{8} g_2^4 \right. \\ & \left. - 6 \text{Tr} \left(Y_u^\dagger Y_u \right)^2 - 2 \text{Tr} \left(Y_\nu^\dagger Y_\nu \right)^2 \right] \end{aligned} \quad (\text{A.12})$$

$$\beta_{\lambda_2, \text{add}}(g_i, y_j, \lambda_k) = \frac{1}{16\pi^2} \left[20 \lambda_2^2 + 2 \lambda_3^2 + 96 g_X^4 - 16 \text{Tr} (Y_N^* Y_N)^2 \right] \quad (\text{A.13})$$

$$\beta_{\lambda_3, \text{add}}(g_i, y_j, \lambda_k) = \frac{1}{16\pi^2} \left[12 \lambda_1 \lambda_3 + 8 \lambda_2 \lambda_3 + 4 \lambda_3^2 + 12 g_X^2 g_\epsilon^2 - 16 \text{Tr} \left(Y_\nu^\dagger Y_\nu Y_N^* Y_N \right) \right] \quad (\text{A.14})$$

$$\beta_{\tilde{m}_H^2, \text{add}}(\tilde{m}_H^2, \tilde{m}_S^2) = \frac{1}{16\pi^2} (12 \lambda_1 \tilde{m}_H^2 + 2 \lambda_3 \tilde{m}_S^2) \quad (\text{A.15})$$

$$\beta_{\tilde{m}_S^2, \text{add}}(\tilde{m}_H^2, \tilde{m}_S^2) = \frac{1}{16\pi^2} (4 \lambda_3 \tilde{m}_H^2 + 8 \lambda_2 \tilde{m}_S^2). \quad (\text{A.16})$$

B Thermally corrected effective potential

The tree-level scalar potential of the $B - L$ model is defined in Eq. (4.4). Since the vev of the scalar S is much larger than the Higgs vev, $vs \gg v_H$ (cf. Sec. 4.2), the $B - L$ phase transition occurs along the S direction. Thus, we can limit our analysis to the S -dependent part of $V(H, S)$. The symmetry of the potential only allows terms in powers of $S^\dagger S$ (the same goes for the SM Higgs scalar), it is then enough to consider the effective potential for the radial component $\phi = \sqrt{2} \text{Re}(S)$,

$$S^\dagger S = \frac{1}{2} \phi^2. \quad (\text{B.1})$$

The tree-level part of the effective potential reads

$$V_0(\phi) = \frac{1}{2} m_S^2 \phi^2 + \frac{1}{4} \lambda_2 \phi^4. \quad (\text{B.2})$$

The finite one-loop Coleman-Weinberg contributions are given by [58]

$$V_{1\text{-loop}}(\phi) = \frac{1}{64\pi^2} \sum_J n_J m_J^4(\phi) \left[\log \frac{m_J^2(\phi)}{\mu^2} - C_J \right], \quad (\text{B.3})$$

where $n_J = (-1)^{2s_J} Q_J N_J (2s_J + 1)$, with $Q_J = 1(2)$ for uncharged (charged) particles, $N_J = 1(3)$ for uncolored (colored) particles, and $C_J = \frac{5}{6} (\frac{3}{2})$ for vector bosons (fermions and scalars); s_J is the particle spin and m_J is the field-dependent mass of the particle. In the $B - L$ model the sum runs over the gauge boson Z' , three right-handed neutrinos $\nu_{R,i}$, the real scalar ϕ and the corresponding Goldstone boson G ,

$$\begin{aligned} V_{1\text{-loop}}(\phi) = & \frac{3}{64\pi^2} m_{Z'}^4(\phi) \left[\log \frac{m_{Z'}^2(\phi)}{\mu^2} - \frac{5}{6} \right] - \frac{2}{64\pi^2} \sum_{i=1}^3 m_{\nu_{R,i}}^4(\phi) \left[\log \frac{m_{\nu_{R,i}}^2(\phi)}{\mu^2} - \frac{3}{2} \right] \\ & + \frac{1}{64\pi^2} m_\phi^4(\phi) \left[\log \frac{m_\phi^2(\phi)}{\mu^2} - \frac{3}{2} \right] + \frac{1}{64\pi^2} m_G^4(\phi) \left[\log \frac{m_G^2(\phi)}{\mu^2} - \frac{3}{2} \right]. \end{aligned} \quad (\text{B.4})$$

The ϕ -dependent masses that enter Eq. (B.4) are obtained from the second derivatives of Eq. (3.17), Eq. (3.18) and Eq. (B.2) and read

$$m_{Z'}^2(\phi) = 4 g_X^2 \phi^2 \quad (\text{B.5})$$

$$m_{\nu_{R,i}}^2(\phi) = 2 y_N^2 \phi^2 \quad (\text{B.6})$$

$$m_\phi^2(\phi) = 3 \lambda_2 \phi^2 + m_S^2 \quad (\text{B.7})$$

$$m_G^2(\phi) = \lambda_2 \phi^2 + m_S^2. \quad (\text{B.8})$$

The finite-temperature one-loop corrections to the effective potential are given by [135, 136]

$$V_{\text{thermal}}(\phi, T) = \frac{T^4}{2\pi^2} \sum_J n_J J_J \left(\frac{m_J^2(\phi)}{T^2} \right), \quad (\text{B.9})$$

and again the sum runs over Z' , $\nu_{R,i}$, ϕ and G . The thermal integrals J_J are defined as

$$J_{B,F}(y) = \int_0^\infty dx x^2 \log \left(1 \mp e^{-\sqrt{x^2+y}} \right), \quad (\text{B.10})$$

where B and F stands for bosons and fermions, respectively. Additionally, the resummed daisy diagrams with the bosonic degrees of freedom contribute as [137]

$$V_{\text{daisy}}(\phi, T) = \frac{T}{12\pi} \sum_J k_J [m_J^3(\phi) - \mathcal{M}_J^3(\phi, T)], \quad (\text{B.11})$$

where $k_{Z'} = k_\phi = k_G = 1$ and thermally corrected (Debye) masses are defined as $\mathcal{M}_J^2(\phi, T) = m_J^2(\phi) + \Pi_J(\phi, T)$, with the temperature-dependent self-energies [106]

$$\Pi_{Z'}(\phi, T) = 4 g_X^2 T^2 \quad (\text{B.12})$$

$$\Pi_\phi(\phi, T) = \left(g_X^2 + \frac{1}{3} \lambda_2 + \frac{1}{2} y_N^2 \right) T^2 \quad (\text{B.13})$$

$$\Pi_G(\phi, T) = \Pi_\phi(\phi, T). \quad (\text{B.14})$$

The total thermally-corrected effective potential for the scalar ϕ thus reads

$$V(\phi, T) = V_0(\phi) + V_{1\text{-loop}}(\phi) + V_{\text{thermal}}(\phi, T) + V_{\text{daisy}}(\phi, T). \quad (\text{B.15})$$

Finally, to mitigate the dependence of our results on the renormalization scale, we implement the RG-improvement of the scalar potential $V(\phi, T)$. We replace all the couplings (collectively denoted with $\{\alpha_i\}$) with the running couplings in the \overline{MS} scheme, $\{\alpha_i\} \rightarrow \{\alpha_i(t)\}$, and we introduce the field strength renormalization constant $\phi \rightarrow \sqrt{Z_\phi(t)} \phi$, with $t = \ln \mu$. After the counterterms are introduced to absorb the infinities arising at one loop, Eq. (B.4) leads straightforwardly to Eq. (4.10).

C Phase transition and gravitational waves

At high temperatures, the potential $V(\phi, T)$ is dominated by thermal corrections and it features a single minimum at $\langle \phi \rangle = 0$. As the Universe cools down, the second minimum with $\langle \phi \rangle \neq 0$ is formed and at the critical temperature, T_c , the two minima reach the same depth. Below T_c , the symmetry-breaking minimum becomes the global one and as the temperature further decreases and a thermal barrier between $\langle \phi \rangle = 0$ and $\langle \phi \rangle \neq 0$ keeps getting lower, tunneling from the false to the true vacuum may take place. A FOPT begins and bubbles of the symmetry-broken phase start to nucleate and grow in the sea of the false vacuum. Its decay rate is given by [111, 112]

$$\Gamma(T) \approx T^4 \left(\frac{S_3(T)}{2\pi T} \right)^{\frac{3}{2}} e^{-S_3(T)/T}. \quad (\text{C.1})$$

In Eq. (C.1) $S_3(T)$ indicates the three-dimensional thermal bounce action along the tunneling path, which we calculate with `CosmoTransitions` [138]. One can now define the nucleation temperature, T_n , as the temperature at which at least one bubble per Hubble volume has nucleated [139],

$$N(T_n) = \int_{T_n}^{T_c} \frac{dT}{T} \frac{\Gamma(T)}{H(T)^4} = 1. \quad (\text{C.2})$$

The Hubble parameter $H(T)$ is defined, *e.g.*, in Eq. (4.10) of Ref. [140]. The fraction of the true vacuum volume at a given temperature, $I(T)$, reads [141–143]

$$I(T) = \frac{4\pi}{3} \int_T^{T_c} dT' \frac{\Gamma(T')}{T'^4 H(T')} \left(\int_T^{T'} dT'' \frac{1}{H(T'')} \right)^3. \quad (\text{C.3})$$

As the number and the size of the true-vacuum bubbles increase, the bubble collisions start to take place and the GW signal is generated. The percolation temperature is then defined as the temperature at which bubbles form an infinitely connected cluster, which corresponds to [139, 144]

$$I(T_p) = 0.34. \quad (\text{C.4})$$

It may happen that the expansion rate of the Universe is faster than the growth of the bubbles. In such a case the percolation would never end and the phase transition would never be completed. To make sure that the entire false vacuum decays, its decay rate must exceed the expansion rate of the Universe. The corresponding condition for successful completion of the phase transition reads [140, 143]

$$3 + T \frac{dI(T)}{dT} \Big|_{T=T_p} < 0. \quad (\text{C.5})$$

The production of GWs from the phase transition occurs around the percolation temperature and all the parameters are evaluated at that temperature. The strength of the signal is determined by the latent heat released during the transition [143],

$$\alpha = \frac{\Delta V(T) - T \frac{\partial \Delta V(T)}{\partial T}}{\rho_R(T)} \Big|_{T_p}, \quad (\text{C.6})$$

where ΔV is the effective potential difference between the false and the true vacuum, while ρ_R denotes the density of radiation given by $\rho_R(T) = g_* T^4 \pi^2/30$, with g_* being the number of degrees of freedom in the plasma.⁵ Another important quantity is the inverse time scale of the transition (in other words, the nucleation speed),

$$\frac{\beta}{H_*} = T_p \frac{d(S_3/T)}{dT} \Big|_{T_p}. \quad (\text{C.7})$$

After the phase transition ends, the energy stored in the vacuum is immediately turned into radiation. Reheating thus takes place, characterized by the temperature [143, 147]

$$T_{\text{rh}} = T_p [1 + \alpha(T_p)]^{1/4}. \quad (\text{C.8})$$

The stochastic gravitational wave background produced at the time of the FOPT can originate from collisions of bubble walls (Ω_{coll}), sound waves in the plasma (Ω_{sw}), and magnetohydrodynamic turbulence in the plasma (Ω_{turb}). The total amplitude of the redshifted signal observed today is then given by

$$h^2 \Omega_{\text{GW}} = h^2 \Omega_{\text{coll}} + h^2 \Omega_{\text{sw}} + h^2 \Omega_{\text{turb}}, \quad (\text{C.9})$$

⁵See also Refs. [145, 146] for a more rigorous definition of α .

where $h = H_0/(100 \text{ km/s/Mpc})$ is the present-day value of the dimensionless Hubble parameter. The corresponding GW spectra are given in terms of the peak amplitudes Ω^{peak} and the peak frequencies f^{peak} as [59–62, 148–163]

$$\begin{aligned} h^2 \Omega_{\text{coll}}(f) &= h^2 \Omega_{\text{coll}}^{\text{peak}} \left(\frac{f}{f_{\text{coll}}^{\text{peak}}} \right)^{2.8} \left(\frac{3.8}{1 + 2.8 (f/f_{\text{coll}}^{\text{peak}})^{3.8}} \right) \\ h^2 \Omega_{\text{sw}}(f) &= h^2 \Omega_{\text{sw}}^{\text{peak}} \left(\frac{f}{f_{\text{sw}}^{\text{peak}}} \right)^3 \left(\frac{7}{4 + 3 (f/f_{\text{sw}}^{\text{peak}})^2} \right)^{7/2} \\ h^2 \Omega_{\text{turb}}(f) &= h^2 \Omega_{\text{turb}}^{\text{peak}} \left(\frac{f}{f_{\text{turb}}^{\text{peak}}} \right)^3 \left(\frac{1}{1 + (f/f_{\text{turb}}^{\text{peak}})} \right)^{11/3} \frac{1}{1 + 8\pi f a_0/a_* H_*}. \end{aligned} \quad (\text{C.10})$$

The red-shifted Hubble parameter reads

$$\frac{a_*}{a_0} H_* = 1.65 \times 10^{-5} \text{ Hz} \left(\frac{g_*}{100} \right)^{1/6} \left(\frac{T_*}{100 \text{ GeV}} \right). \quad (\text{C.11})$$

In Eq. (C.11), T_* is the temperature of the plasma at the time of the GW production, after the transition has completed and reheating has taken place, which will be identified with the reheating temperature, $T_* = T_{\text{rh}}$. The peak amplitude for each source of GW is given by

$$\begin{aligned} h^2 \Omega_{\text{coll}}^{\text{peak}} &= 1.67 \times 10^{-5} \kappa_{\text{coll}}^2 \left(\frac{\alpha}{1 + \alpha} \right)^2 \left(\frac{v_w}{\beta/H_*} \right)^2 \left(\frac{100}{g_*} \right)^{1/3} \left(\frac{0.11 v_w}{0.42 + v_w^2} \right) \\ h^2 \Omega_{\text{sw}}^{\text{peak}} &= 2.65 \times 10^{-6} \kappa_{\text{sw}}^2 \left(\frac{\alpha}{1 + \alpha} \right)^2 \left(\frac{v_w}{\beta/H_*} \right) \left(\frac{100}{g_*} \right)^{1/3} \\ h^2 \Omega_{\text{turb}}^{\text{peak}} &= 3.35 \times 10^{-4} \kappa_{\text{turb}}^{3/2} \left(\frac{\alpha}{1 + \alpha} \right)^{3/2} \left(\frac{v_w}{\beta/H_*} \right) \left(\frac{100}{g_*} \right)^{1/3}, \end{aligned} \quad (\text{C.12})$$

where v_w is the bubble wall velocity assumed to be equal to the speed of light, $v_w = 1$ (the effects of a smaller wall velocity were discussed in Ref. [164]). The parameters κ_{coll} , κ_{sw} and κ_{turb} are the efficiency factors that indicate the amount of the released vacuum energy converted into the energy of the bubble wall, sound waves and turbulence, respectively, defined in Ref. [165]. Finally, the peak frequencies read

$$\begin{aligned} f_{\text{coll}}^{\text{peak}} &= 1.65 \times 10^{-5} \text{ Hz} \left(\frac{v_w}{\beta/H_*} \right)^{-1} \left(\frac{100}{g_*} \right)^{-1/6} \left(\frac{T_*}{100 \text{ GeV}} \right) \left(\frac{0.62 v_w}{1.81 - 0.1 v_w + v_w^2} \right) \\ f_{\text{sw}}^{\text{peak}} &= 1.90 \times 10^{-5} \text{ Hz} \left(\frac{v_w}{\beta/H_*} \right)^{-1} \left(\frac{100}{g_*} \right)^{-1/6} \left(\frac{T_*}{100 \text{ GeV}} \right) \\ f_{\text{turb}}^{\text{peak}} &= 2.70 \times 10^{-5} \text{ Hz} \left(\frac{v_w}{\beta/H_*} \right)^{-1} \left(\frac{100}{g_*} \right)^{-1/6} \left(\frac{T_*}{100 \text{ GeV}} \right). \end{aligned} \quad (\text{C.13})$$

References

- [1] P. Minkowski, $\mu \rightarrow e\gamma$ at a Rate of One Out of 10^9 Muon Decays?, *Phys. Lett. B* **67** (1977) 421–428.

- [2] M. Gell-Mann, P. Ramond, and R. Slansky, *Complex Spinors and Unified Theories*, *Conf. Proc. C* **790927** (1979) 315–321, [[arXiv:1306.4669](#)].
- [3] T. Yanagida, *Horizontal gauge symmetry and masses of neutrinos*, *Conf. Proc. C* **7902131** (1979) 95–99.
- [4] S. L. Glashow, *The Future of Elementary Particle Physics*, *NATO Sci. Ser. B* **61** (1980) 687.
- [5] R. N. Mohapatra and G. Senjanovic, *Neutrino Masses and Mixings in Gauge Models with Spontaneous Parity Violation*, *Phys. Rev. D* **23** (1981) 165.
- [6] J. Schechter and J. W. F. Valle, *Neutrino Decay and Spontaneous Violation of Lepton Number*, *Phys. Rev. D* **25** (1982) 774.
- [7] J. Schechter and J. W. F. Valle, *Neutrino Masses in $SU(2) \times U(1)$ Theories*, *Phys. Rev. D* **22** (1980) 2227.
- [8] Y. Cai, J. Herrero-García, M. A. Schmidt, A. Vicente, and R. R. Volkas, *From the trees to the forest: a review of radiative neutrino mass models*, *Front. in Phys.* **5** (2017) 63, [[arXiv:1706.08524](#)].
- [9] C. Klein, M. Lindner, and S. Ohmer, *Minimal Radiative Neutrino Masses*, *JHEP* **03** (2019) 018, [[arXiv:1901.03225](#)].
- [10] K. Kowalska, S. Pramanick, and E. M. Sessolo, *Naturally small Yukawa couplings from trans-Planckian asymptotic safety*, *JHEP* **08** (2022) 262, [[arXiv:2204.00866](#)].
- [11] A. Eichhorn and A. Held, *Dynamically vanishing Dirac neutrino mass from quantum scale symmetry*, *Phys. Lett. B* **846** (2023) 138196, [[arXiv:2204.09008](#)].
- [12] F. Deppisch and J. W. F. Valle, *Enhanced lepton flavor violation in the supersymmetric inverse seesaw model*, *Phys. Rev. D* **72** (2005) 036001, [[hep-ph/0406040](#)].
- [13] A. Abada and M. Lucente, *Looking for the minimal inverse seesaw realisation*, *Nucl. Phys. B* **885** (2014) 651–678, [[arXiv:1401.1507](#)].
- [14] M. Lindner, S. Schmidt, and J. Smirnov, *Neutrino Masses and Conformal Electro-Weak Symmetry Breaking*, *JHEP* **10** (2014) 177, [[arXiv:1405.6204](#)].
- [15] S. Weinberg, *General Relativity*, pp. 790–831. S.W.Hawking, W.Israel (Eds.), Cambridge Univ. Press, 1980.
- [16] C. Wetterich, *Exact evolution equation for the effective potential*, *Physics Letters B* **301** (1993), no. 1 90 – 94.
- [17] T. R. Morris, *The Exact renormalization group and approximate solutions*, *Int. J. Mod. Phys. A* **9** (1994) 2411–2450, [[hep-ph/9308265](#)].
- [18] M. Reuter, *Nonperturbative evolution equation for quantum gravity*, *Phys. Rev. D* **57** (1998) 971–985, [[hep-th/9605030](#)].
- [19] O. Lauscher and M. Reuter, *Ultraviolet fixed point and generalized flow equation of quantum gravity*, *Phys. Rev. D* **65** (2002) 025013, [[hep-th/0108040](#)].
- [20] M. Reuter and F. Saueressig, *Renormalization group flow of quantum gravity in the Einstein-Hilbert truncation*, *Phys. Rev. D* **65** (2002) 065016, [[hep-th/0110054](#)].
- [21] O. Lauscher and M. Reuter, *Flow equation of quantum Einstein gravity in a higher derivative truncation*, *Phys. Rev. D* **66** (2002) 025026, [[hep-th/0205062](#)].

- [22] D. F. Litim, *Fixed points of quantum gravity*, *Phys. Rev. Lett.* **92** (2004) 201301, [[hep-th/0312114](#)].
- [23] A. Codello and R. Percacci, *Fixed points of higher derivative gravity*, *Phys. Rev. Lett.* **97** (2006) 221301, [[hep-th/0607128](#)].
- [24] P. F. Machado and F. Saueressig, *On the renormalization group flow of $f(R)$ -gravity*, *Phys. Rev. D* **77** (2008) 124045, [[arXiv:0712.0445](#)].
- [25] A. Codello, R. Percacci, and C. Rahmede, *Investigating the Ultraviolet Properties of Gravity with a Wilsonian Renormalization Group Equation*, *Annals Phys.* **324** (2009) 414–469, [[arXiv:0805.2909](#)].
- [26] D. Benedetti, P. F. Machado, and F. Saueressig, *Asymptotic safety in higher-derivative gravity*, *Mod. Phys. Lett. A* **24** (2009) 2233–2241, [[arXiv:0901.2984](#)].
- [27] J. A. Dietz and T. R. Morris, *Asymptotic safety in the $f(R)$ approximation*, *JHEP* **01** (2013) 108, [[arXiv:1211.0955](#)].
- [28] K. Falls, D. Litim, K. Nikolakopoulos, and C. Rahmede, *A bootstrap towards asymptotic safety*, [[arXiv:1301.4191](#)].
- [29] K. Falls, D. F. Litim, K. Nikolakopoulos, and C. Rahmede, *Further evidence for asymptotic safety of quantum gravity*, *Phys. Rev. D* **93** (2016), no. 10 104022, [[arXiv:1410.4815](#)].
- [30] K.-y. Oda and M. Yamada, *Non-minimal coupling in Higgs–Yukawa model with asymptotically safe gravity*, *Class. Quant. Grav.* **33** (2016), no. 12 125011, [[arXiv:1510.03734](#)].
- [31] Y. Hamada and M. Yamada, *Asymptotic safety of higher derivative quantum gravity non-minimally coupled with a matter system*, *JHEP* **08** (2017) 070, [[arXiv:1703.09033](#)].
- [32] N. Christiansen, D. F. Litim, J. M. Pawłowski, and M. Reichert, *Asymptotic safety of gravity with matter*, *Phys. Rev. D* **97** (2018), no. 10 106012, [[arXiv:1710.04669](#)].
- [33] S. P. Robinson and F. Wilczek, *Gravitational correction to running of gauge couplings*, *Phys. Rev. Lett.* **96** (2006) 231601, [[hep-th/0509050](#)].
- [34] A. R. Pietrykowski, *Gauge dependence of gravitational correction to running of gauge couplings*, *Phys. Rev. Lett.* **98** (2007) 061801, [[hep-th/0606208](#)].
- [35] D. J. Toms, *Quantum gravity and charge renormalization*, *Phys. Rev. D* **76** (2007) 045015, [[arXiv:0708.2990](#)].
- [36] Y. Tang and Y.-L. Wu, *Gravitational Contributions to the Running of Gauge Couplings*, *Commun. Theor. Phys.* **54** (2010) 1040–1044, [[arXiv:0807.0331](#)].
- [37] D. J. Toms, *Cosmological constant and quantum gravitational corrections to the running fine structure constant*, *Phys. Rev. Lett.* **101** (2008) 131301, [[arXiv:0809.3897](#)].
- [38] A. Rodigast and T. Schuster, *Gravitational Corrections to Yukawa and ϕ^4 Interactions*, *Phys. Rev. Lett.* **104** (2010) 081301, [[arXiv:0908.2422](#)].
- [39] O. Zanusso, L. Zambelli, G. Vacca, and R. Percacci, *Gravitational corrections to Yukawa systems*, *Phys. Lett. B* **689** (2010) 90–94, [[arXiv:0904.0938](#)].
- [40] J.-E. Daum, U. Harst, and M. Reuter, *Running Gauge Coupling in Asymptotically Safe Quantum Gravity*, *JHEP* **01** (2010) 084, [[arXiv:0910.4938](#)].

- [41] J.-E. Daum, U. Harst, and M. Reuter, *Non-perturbative QEG Corrections to the Yang-Mills Beta Function*, *Gen. Rel. Grav.* **43** (2011) 2393, [[arXiv:1005.1488](#)].
- [42] S. Folkerts, D. F. Litim, and J. M. Pawłowski, *Asymptotic freedom of Yang-Mills theory with gravity*, *Phys. Lett. B* **709** (2012) 234–241, [[arXiv:1101.5552](#)].
- [43] A. Eichhorn, A. Held, and J. M. Pawłowski, *Quantum-gravity effects on a Higgs-Yukawa model*, *Phys. Rev. D* **94** (2016), no. 10 104027, [[arXiv:1604.02041](#)].
- [44] A. Eichhorn and A. Held, *Viability of quantum-gravity induced ultraviolet completions for matter*, *Phys. Rev. D* **96** (2017), no. 8 086025, [[arXiv:1705.02342](#)].
- [45] U. Harst and M. Reuter, *QED coupled to QEG*, *JHEP* **05** (2011) 119, [[arXiv:1101.6007](#)].
- [46] N. Christiansen and A. Eichhorn, *An asymptotically safe solution to the $U(1)$ triviality problem*, *Phys. Lett. B* **770** (2017) 154–160, [[arXiv:1702.07724](#)].
- [47] A. Eichhorn and F. Versteegen, *Upper bound on the Abelian gauge coupling from asymptotic safety*, *JHEP* **01** (2018) 030, [[arXiv:1709.07252](#)].
- [48] M. Shaposhnikov and C. Wetterich, *Asymptotic safety of gravity and the Higgs boson mass*, *Phys. Lett. B* **683** (2010) 196–200, [[arXiv:0912.0208](#)].
- [49] A. Eichhorn, Y. Hamada, J. Lumma, and M. Yamada, *Quantum gravity fluctuations flatten the Planck-scale Higgs potential*, *Phys. Rev. D* **97** (2018), no. 8 086004, [[arXiv:1712.00319](#)].
- [50] J. H. Kwapisz, *Asymptotic safety, the Higgs boson mass, and beyond the standard model physics*, *Phys. Rev. D* **100** (2019), no. 11 115001, [[arXiv:1907.12521](#)].
- [51] A. Eichhorn, M. Pauly, and S. Ray, *Towards a Higgs mass determination in asymptotically safe gravity with a dark portal*, *JHEP* **10** (2021) 100, [[arXiv:2107.07949](#)].
- [52] A. Eichhorn and A. Held, *Top mass from asymptotic safety*, *Phys. Lett. B* **777** (2018) 217–221, [[arXiv:1707.01107](#)].
- [53] E. E. Jenkins, *Searching for a $(B-l)$ Gauge Boson in $p\bar{p}$ Collisions*, *Phys. Lett. B* **192** (1987) 219–222.
- [54] W. Buchmüller, C. Greub, and P. Minkowski, *Neutrino masses, neutral vector bosons and the scale of $B-L$ breaking*, *Phys. Lett. B* **267** (1991) 395–399.
- [55] K. Falls, D. F. Litim, and A. Raghuraman, *Black Holes and Asymptotically Safe Gravity*, *Int. J. Mod. Phys. A* **27** (2012) 1250019, [[arXiv:1002.0260](#)].
- [56] Y. Aharonov, A. Casher, and S. Nussinov, *The Unitarity Puzzle and Planck Mass Stable Particles*, *Phys. Lett. B* **191** (1987) 51.
- [57] T. Banks, A. Dabholkar, M. R. Douglas, and M. O’Loughlin, *Are horned particles the climax of Hawking evaporation?*, *Phys. Rev. D* **45** (1992) 3607–3616, [[hep-th/9201061](#)].
- [58] S. Coleman and E. Weinberg, *Radiative corrections as the origin of spontaneous symmetry breaking*, *Phys. Rev. D* **7** (Mar, 1973) 1888–1910.
- [59] A. Kosowsky, M. S. Turner, and R. Watkins, *Gravitational radiation from colliding vacuum bubbles*, *Phys. Rev. D* **45** (Jun, 1992) 4514–4535.
- [60] A. Kosowsky, M. S. Turner, and R. Watkins, *Gravitational waves from first-order cosmological phase transitions*, *Phys. Rev. Lett.* **69** (Oct, 1992) 2026–2029.

- [61] A. Kosowsky and M. S. Turner, *Gravitational radiation from colliding vacuum bubbles: envelope approximation to many bubble collisions*, *Phys. Rev. D* **47** (1993) 4372–4391, [[astro-ph/9211004](#)].
- [62] M. Kamionkowski, A. Kosowsky, and M. S. Turner, *Gravitational radiation from first order phase transitions*, *Phys. Rev. D* **49** (1994) 2837–2851, [[astro-ph/9310044](#)].
- [63] P. Athron, C. Balázs, A. Fowlie, L. Morris, and L. Wu, *Cosmological phase transitions: from perturbative particle physics to gravitational waves*, [arXiv:2305.02357](#).
- [64] R. Percacci and D. Perini, *Constraints on matter from asymptotic safety*, *Phys. Rev. D* **67** (2003) 081503, [[hep-th/0207033](#)].
- [65] R. Percacci and D. Perini, *Asymptotic safety of gravity coupled to matter*, *Phys. Rev. D* **68** (2003) 044018, [[hep-th/0304222](#)].
- [66] A. Codello, R. Percacci, and C. Rahmede, *Ultraviolet properties of $f(R)$ -gravity*, *Int. J. Mod. Phys. A* **23** (2008) 143–150, [[arXiv:0705.1769](#)].
- [67] G. Narain and R. Percacci, *On the scheme dependence of gravitational beta functions*, *Acta Phys. Polon. B* **40** (2009) 3439–3457, [[arXiv:0910.5390](#)].
- [68] P. Donà, A. Eichhorn, and R. Percacci, *Matter matters in asymptotically safe quantum gravity*, *Phys. Rev. D* **89** (2014), no. 8 084035, [[arXiv:1311.2898](#)].
- [69] K. Falls, C. R. King, D. F. Litim, K. Nikolakopoulos, and C. Rahmede, *Asymptotic safety of quantum gravity beyond Ricci scalars*, *Phys. Rev. D* **97** (2018), no. 8 086006, [[arXiv:1801.00162](#)].
- [70] K. G. Falls, D. F. Litim, and J. Schröder, *Aspects of asymptotic safety for quantum gravity*, *Phys. Rev. D* **99** (2019), no. 12 126015, [[arXiv:1810.08550](#)].
- [71] A. Pastor-Gutiérrez, J. M. Pawłowski, and M. Reichert, *The Asymptotically Safe Standard Model: From quantum gravity to dynamical chiral symmetry breaking*, *SciPost Phys.* **15** (2023) 105, [[arXiv:2207.09817](#)].
- [72] W. Kotlarski, K. Kowalska, D. Rizzo, and E. M. Sessolo, *How robust are particle physics predictions in asymptotic safety?*, *Eur. Phys. J. C* **83** (2023), no. 7 644, [[arXiv:2304.08959](#)].
- [73] A. Eichhorn and M. Pauly, *Safety in darkness: Higgs portal to simple Yukawa systems*, *Phys. Lett. B* **819** (2021) 136455, [[arXiv:2005.03661](#)].
- [74] A. Eichhorn and A. Held, *Mass difference for charged quarks from asymptotically safe quantum gravity*, *Phys. Rev. Lett.* **121** (2018), no. 15 151302, [[arXiv:1803.04027](#)].
- [75] R. Alkofer, A. Eichhorn, A. Held, C. M. Nieto, R. Percacci, and M. Schröfl, *Quark masses and mixings in minimally parameterized UV completions of the Standard Model*, *Annals Phys.* **421** (2020) 168282, [[arXiv:2003.08401](#)].
- [76] G. P. De Brito, Y. Hamada, A. D. Pereira, and M. Yamada, *On the impact of Majorana masses in gravity-matter systems*, *JHEP* **08** (2019) 142, [[arXiv:1905.11114](#)].
- [77] Y. Hamada, K. Tsumura, and M. Yamada, *Scalegenesis and fermionic dark matters in the flatland scenario*, *Eur. Phys. J. C* **80** (2020), no. 5 368, [[arXiv:2002.03666](#)].
- [78] G. Domènech, M. Goodsell, and C. Wetterich, *Neutrino masses, vacuum stability and quantum gravity prediction for the mass of the top quark*, *JHEP* **01** (2021) 180, [[arXiv:2008.04310](#)].

- [79] F. Grabowski, J. H. Kwapisz, and K. A. Meissner, *Asymptotic safety and Conformal Standard Model*, *Phys. Rev. D* **99** (2019), no. 11 115029, [[arXiv:1810.08461](#)].
- [80] K. Kowalska, E. M. Sessolo, and Y. Yamamoto, *Flavor anomalies from asymptotically safe gravity*, *Eur. Phys. J. C* **81** (2021), no. 4 272, [[arXiv:2007.03567](#)].
- [81] A. Chikkaballi, W. Kotlarski, K. Kowalska, D. Rizzo, and E. M. Sessolo, *Constraints on Z' solutions to the flavor anomalies with trans-Planckian asymptotic safety*, *JHEP* **01** (2023) 164, [[arXiv:2209.07971](#)].
- [82] K. Kowalska and E. M. Sessolo, *Minimal models for $g-2$ and dark matter confront asymptotic safety*, *Phys. Rev. D* **103** (2021), no. 11 115032, [[arXiv:2012.15200](#)].
- [83] M. Reichert and J. Smirnov, *Dark Matter meets Quantum Gravity*, *Phys. Rev. D* **101** (2020), no. 6 063015, [[arXiv:1911.00012](#)].
- [84] J. Boos, C. D. Carone, N. L. Donald, and M. R. Musser, *Asymptotic safety and gauged baryon number*, *Phys. Rev. D* **106** (2022), no. 3 035015, [[arXiv:2206.02686](#)].
- [85] J. Boos, C. D. Carone, N. L. Donald, and M. R. Musser, *Asymptotically safe dark matter with gauged baryon number*, *Phys. Rev. D* **107** (2023), no. 3 035018, [[arXiv:2209.14268](#)].
- [86] G. P. de Brito, A. Eichhorn, and R. R. Lino dos Santos, *Are there ALPs in the asymptotically safe landscape?*, *JHEP* **06** (2022) 013, [[arXiv:2112.08972](#)].
- [87] A. Eichhorn, R. R. Lino dos Santos, and J. a. L. Miqueleto, *From quantum gravity to gravitational waves through cosmic strings*, [arXiv:2306.17718](#).
- [88] C. Coriano, L. Delle Rose, and C. Marzo, *Constraints on abelian extensions of the Standard Model from two-loop vacuum stability and $U(1)_{B-L}$* , *JHEP* **02** (2016) 135, [[arXiv:1510.02379](#)].
- [89] F. Lyonnet and I. Schienbein, *PyR@TE 2: A Python tool for computing RGEs at two-loop*, *Comput. Phys. Commun.* **213** (2017) 181–196, [[arXiv:1608.07274](#)].
- [90] B. Holdom, *Two $U(1)$'s and Epsilon Charge Shifts*, *Phys. Lett. B* **166** (1986) 196–198.
- [91] K. S. Babu, C. F. Kolda, and J. March-Russell, *Leptophobic $U(1)$ s and the $R(b) - R(c)$ crisis*, *Phys. Rev. D* **54** (1996) 4635–4647, [[hep-ph/9603212](#)].
- [92] **ATLAS** Collaboration, G. Aad et al., *Search for high-mass dilepton resonances using 139 fb^{-1} of pp collision data collected at $\sqrt{s}=13\text{ TeV}$ with the ATLAS detector*, *Phys. Lett. B* **796** (2019) 68–87, [[arXiv:1903.06248](#)].
- [93] **CMS** Collaboration, A. M. Sirunyan et al., *Search for resonant and nonresonant new phenomena in high-mass dilepton final states at $\sqrt{s} = 13\text{ TeV}$* , *JHEP* **07** (2021) 208, [[arXiv:2103.02708](#)].
- [94] **Particle Data Group** Collaboration, R. L. Workman and Others, *Review of Particle Physics*, *PTEP* **2022** (2022) 083C01.
- [95] R. Hempfling, *The Next-to-minimal Coleman-Weinberg model*, *Phys. Lett. B* **379** (1996) 153–158, [[hep-ph/9604278](#)].
- [96] M. Sher, *The Coleman-Weinberg phase transition in extended Higgs models*, *Phys. Rev. D* **54** (1996) 7071–7074, [[hep-ph/9607337](#)].
- [97] H. Nishino and S. Rajpoot, *Broken scale invariance in the standard model*, [hep-th/0403039](#).

- [98] K. A. Meissner and H. Nicolai, *Conformal Symmetry and the Standard Model*, *Phys. Lett. B* **648** (2007) 312–317, [[hep-th/0612165](#)].
- [99] S. Iso, N. Okada, and Y. Orikasa, *Classically conformal $B-L$ extended Standard Model*, *Phys. Lett. B* **676** (2009) 81–87, [[arXiv:0902.4050](#)].
- [100] C. Wetterich and M. Yamada, *Gauge hierarchy problem in asymptotically safe gravity—the resurgence mechanism*, *Phys. Lett. B* **770** (2017) 268–271, [[arXiv:1612.03069](#)].
- [101] J. M. Pawłowski, M. Reichert, C. Wetterich, and M. Yamada, *Higgs scalar potential in asymptotically safe quantum gravity*, *Phys. Rev. D* **99** (2019), no. 8 086010, [[arXiv:1811.11706](#)].
- [102] C. Wetterich and M. Yamada, *Variable Planck mass from the gauge invariant flow equation*, *Phys. Rev. D* **100** (2019), no. 6 066017, [[arXiv:1906.01721](#)].
- [103] R. Jinno and M. Takimoto, *Probing a classically conformal $B-L$ model with gravitational waves*, *Phys. Rev. D* **95** (2017), no. 1 015020, [[arXiv:1604.05035](#)].
- [104] W. Chao, W.-F. Cui, H.-K. Guo, and J. Shu, *Gravitational wave imprint of new symmetry breaking*, *Chin. Phys. C* **44** (2020), no. 12 123102, [[arXiv:1707.09759](#)].
- [105] N. Okada and O. Seto, *Probing the seesaw scale with gravitational waves*, *Phys. Rev. D* **98** (2018), no. 6 063532, [[arXiv:1807.00336](#)].
- [106] C. Marzo, L. Marzola, and V. Vaskonen, *Phase transition and vacuum stability in the classically conformal $B-L$ model*, *Eur. Phys. J. C* **79** (2019), no. 7 601, [[arXiv:1811.11169](#)].
- [107] V. Brdar, A. J. Helmboldt, and J. Kubo, *Gravitational Waves from First-Order Phase Transitions: LIGO as a Window to Unexplored Seesaw Scales*, *JCAP* **02** (2019) 021, [[arXiv:1810.12306](#)].
- [108] T. Hasegawa, N. Okada, and O. Seto, *Gravitational waves from the minimal gauged $U(1)_{B-L}$ model*, *Phys. Rev. D* **99** (2019), no. 9 095039, [[arXiv:1904.03020](#)].
- [109] S. Weinberg, *Gauge and global symmetries at high temperature*, *Phys. Rev. D* **9** (Jun, 1974) 3357–3378.
- [110] L. Dolan and R. Jackiw, *Symmetry behavior at finite temperature*, *Phys. Rev. D* **9** (Jun, 1974) 3320–3341.
- [111] A. Linde, *Fate of the false vacuum at finite temperature: Theory and applications*, *Physics Letters B* **100** (1981), no. 1 37–40.
- [112] A. Linde, *Decay of the false vacuum at finite temperature*, *Nuclear Physics B* **216** (1983), no. 2 421–445.
- [113] T. Hambye and A. Strumia, *Dynamical generation of the weak and Dark Matter scale*, *Phys. Rev. D* **88** (2013) 055022, [[arXiv:1306.2329](#)].
- [114] K. Hashino, M. Kakizaki, S. Kanemura, and T. Matsui, *Synergy between measurements of gravitational waves and the triple-Higgs coupling in probing the first-order electroweak phase transition*, *Phys. Rev. D* **94** (2016), no. 1 015005, [[arXiv:1604.02069](#)].
- [115] L. Marzola, A. Racioppi, and V. Vaskonen, *Phase transition and gravitational wave phenomenology of scalar conformal extensions of the Standard Model*, *Eur. Phys. J. C* **77** (2017), no. 7 484, [[arXiv:1704.01034](#)].
- [116] Z. Kang and J. Zhu, *Scale-genesis by Dark Matter and Its Gravitational Wave Signal*, *Phys. Rev. D* **102** (2020), no. 5 053011, [[arXiv:2003.02465](#)].

- [117] A. Dasgupta, P. S. B. Dev, A. Ghoshal, and A. Mazumdar, *Gravitational wave pathway to testable leptogenesis*, *Phys. Rev. D* **106** (2022), no. 7 075027, [[arXiv:2206.07032](#)].
- [118] J. Crowder and N. J. Cornish, *Beyond LISA: Exploring future gravitational wave missions*, *Phys. Rev. D* **72** (2005) 083005, [[gr-qc/0506015](#)].
- [119] V. Corbin and N. J. Cornish, *Detecting the cosmic gravitational wave background with the big bang observer*, *Class. Quant. Grav.* **23** (2006) 2435–2446, [[gr-qc/0512039](#)].
- [120] D. Reitze et al., *Cosmic Explorer: The U.S. Contribution to Gravitational-Wave Astronomy beyond LIGO*, *Bull. Am. Astron. Soc.* **51** (2019), no. 7 035, [[arXiv:1907.04833](#)].
- [121] N. Seto, S. Kawamura, and T. Nakamura, *Possibility of direct measurement of the acceleration of the universe using 0.1-Hz band laser interferometer gravitational wave antenna in space*, *Phys. Rev. Lett.* **87** (2001) 221103, [[astro-ph/0108011](#)].
- [122] **DECIGO Working group** Collaboration, M. Musha, *Space gravitational wave detector DECIGO/pre-DECIGO*, *Proc. SPIE Int. Soc. Opt. Eng.* **10562** (2017) 105623T.
- [123] M. Punturo et al., *The Einstein Telescope: A third-generation gravitational wave observatory*, *Class. Quant. Grav.* **27** (2010) 194002.
- [124] B. Sathyaprakash et al., *Scientific Objectives of Einstein Telescope*, *Class. Quant. Grav.* **29** (2012) 124013, [[arXiv:1206.0331](#)]. [Erratum: *Class. Quant. Grav.* **30**, 079501 (2013)].
- [125] **LIGO Scientific** Collaboration, G. M. Harry, *Advanced LIGO: The next generation of gravitational wave detectors*, *Class. Quant. Grav.* **27** (2010) 084006.
- [126] **LIGO Scientific** Collaboration, J. Aasi et al., *Advanced LIGO*, *Class. Quant. Grav.* **32** (2015) 074001, [[arXiv:1411.4547](#)].
- [127] **LIGO Scientific** Collaboration, B. P. Abbott et al., *Exploring the Sensitivity of Next Generation Gravitational Wave Detectors*, *Class. Quant. Grav.* **34** (2017), no. 4 044001, [[arXiv:1607.08697](#)].
- [128] **LISA** Collaboration, P. Amaro-Seoane et al., *Laser Interferometer Space Antenna*, [arXiv:1702.00786](#).
- [129] J. Baker et al., *The Laser Interferometer Space Antenna: Unveiling the Millihertz Gravitational Wave Sky*, [arXiv:1907.06482](#).
- [130] A. Renzini and C. Contaldi, *Improved limits on a stochastic gravitational-wave background and its anisotropies from Advanced LIGO O1 and O2 runs*, *Phys. Rev. D* **100** (2019), no. 6 063527, [[arXiv:1907.10329](#)].
- [131] **KAGRA, Virgo, LIGO Scientific** Collaboration, R. Abbott et al., *Upper limits on the isotropic gravitational-wave background from Advanced LIGO and Advanced Virgo’s third observing run*, *Phys. Rev. D* **104** (2021), no. 2 022004, [[arXiv:2101.12130](#)].
- [132] S. F. King, D. Marfatia, and M. H. Rahat, *Towards distinguishing Dirac from Majorana neutrino mass with gravitational waves*, [arXiv:2306.05389](#).
- [133] C. Poole and A. E. Thomsen, *Constraints on 3- and 4-loop β -functions in a general four-dimensional Quantum Field Theory*, *JHEP* **09** (2019) 055, [[arXiv:1906.04625](#)].
- [134] L. Sartore and I. Schienbein, *PyR@TE 3*, *Comput. Phys. Commun.* **261** (2021) 107819, [[arXiv:2007.12700](#)].
- [135] M. Quiros, *Finite temperature field theory and phase transitions*, in *ICTP Summer School in High-Energy Physics and Cosmology*, pp. 187–259, 1, 1999. [hep-ph/9901312](#).

- [136] M. Quiros, *Field theory at finite temperature and phase transitions*, *Helv. Phys. Acta* **67** (1994) 451–583.
- [137] P. B. Arnold and O. Espinosa, *The Effective potential and first order phase transitions: Beyond leading-order*, *Phys. Rev. D* **47** (1993) 3546, [[hep-ph/9212235](#)]. [Erratum: *Phys.Rev.D* 50, 6662 (1994)].
- [138] C. L. Wainwright, *CosmoTransitions: Computing Cosmological Phase Transition Temperatures and Bubble Profiles with Multiple Fields*, *Comput. Phys. Commun.* **183** (2012) 2006–2013, [[arXiv:1109.4189](#)].
- [139] M. S. Turner, E. J. Weinberg, and L. M. Widrow, *Bubble nucleation in first-order inflation and other cosmological phase transitions*, *Phys. Rev. D* **46** (Sep, 1992) 2384–2403.
- [140] M. Kierkla, A. Karam, and B. Swiezewska, *Conformal model for gravitational waves and dark matter: a status update*, *JHEP* **03** (2023) 007, [[arXiv:2210.07075](#)].
- [141] A. H. Guth and E. J. Weinberg, *Cosmological consequences of a first-order phase transition in the su_5 grand unified model*, *Phys. Rev. D* **23** (Feb, 1981) 876–885.
- [142] A. H. Guth and S. H. H. Tye, *Phase transitions and magnetic monopole production in the very early universe*, *Phys. Rev. Lett.* **44** (Mar, 1980) 631–635.
- [143] J. Ellis, M. Lewicki, and J. M. No, *On the Maximal Strength of a First-Order Electroweak Phase Transition and its Gravitational Wave Signal*, *JCAP* **04** (2019) 003, [[arXiv:1809.08242](#)].
- [144] M. D. Rintoul and S. Torquato, *Precise determination of the critical threshold and exponents in a three-dimensional continuum percolation model*, *Journal of Physics A: Mathematical and General* **30** (aug, 1997) L585.
- [145] F. Giese, T. Konstandin, and J. van de Vis, *Model-independent energy budget of cosmological first-order phase transitions—A sound argument to go beyond the bag model*, *JCAP* **07** (2020), no. 07 057, [[arXiv:2004.06995](#)].
- [146] F. Giese, T. Konstandin, K. Schmitz, and J. van de Vis, *Model-independent energy budget for LISA*, *JCAP* **01** (2021) 072, [[arXiv:2010.09744](#)].
- [147] A. Eichhorn, J. Lumma, J. M. Pawłowski, M. Reichert, and M. Yamada, *Universal gravitational-wave signatures from heavy new physics in the electroweak sector*, *JCAP* **05** (2021) 006, [[arXiv:2010.00017](#)].
- [148] C. Caprini, R. Durrer, and G. Servant, *Gravitational wave generation from bubble collisions in first-order phase transitions: An analytic approach*, *Phys. Rev. D* **77** (2008) 124015, [[arXiv:0711.2593](#)].
- [149] G. Gogoberidze, T. Kahniashvili, and A. Kosowsky, *The Spectrum of Gravitational Radiation from Primordial Turbulence*, *Phys. Rev. D* **76** (2007) 083002, [[arXiv:0705.1733](#)].
- [150] S. J. Huber and T. Konstandin, *Gravitational Wave Production by Collisions: More Bubbles*, *JCAP* **09** (2008) 022, [[arXiv:0806.1828](#)].
- [151] T. Kahniashvili, L. Campanelli, G. Gogoberidze, Y. Maravin, and B. Ratra, *Gravitational Radiation from Primordial Helical Inverse Cascade MHD Turbulence*, *Phys. Rev. D* **78** (2008) 123006, [[arXiv:0809.1899](#)]. [Erratum: *Phys.Rev.D* 79, 109901 (2009)].
- [152] T. Kahniashvili, L. Kisslinger, and T. Stevens, *Gravitational Radiation Generated by*

Magnetic Fields in Cosmological Phase Transitions, *Phys. Rev. D* **81** (2010) 023004, [[arXiv:0905.0643](#)].

- [153] C. Caprini, R. Durrer, T. Konstandin, and G. Servant, *General Properties of the Gravitational Wave Spectrum from Phase Transitions*, *Phys. Rev. D* **79** (2009) 083519, [[arXiv:0901.1661](#)].
- [154] C. Caprini, R. Durrer, and G. Servant, *The stochastic gravitational wave background from turbulence and magnetic fields generated by a first-order phase transition*, *JCAP* **12** (2009) 024, [[arXiv:0909.0622](#)].
- [155] J. R. Espinosa, T. Konstandin, J. M. No, and G. Servant, *Energy Budget of Cosmological First-order Phase Transitions*, *JCAP* **06** (2010) 028, [[arXiv:1004.4187](#)].
- [156] M. Hindmarsh, S. J. Huber, K. Rummukainen, and D. J. Weir, *Gravitational waves from the sound of a first order phase transition*, *Phys. Rev. Lett.* **112** (2014) 041301, [[arXiv:1304.2433](#)].
- [157] J. T. Giblin and J. B. Mertens, *Gravitational radiation from first-order phase transitions in the presence of a fluid*, *Phys. Rev. D* **90** (2014), no. 2 023532, [[arXiv:1405.4005](#)].
- [158] T. Kalaydzhyan and E. Shuryak, *Gravity waves generated by sounds from big bang phase transitions*, *Phys. Rev. D* **91** (2015), no. 8 083502, [[arXiv:1412.5147](#)].
- [159] M. Hindmarsh, S. J. Huber, K. Rummukainen, and D. J. Weir, *Numerical simulations of acoustically generated gravitational waves at a first order phase transition*, *Phys. Rev. D* **92** (2015), no. 12 123009, [[arXiv:1504.03291](#)].
- [160] C. Caprini et al., *Science with the space-based interferometer eLISA. II: Gravitational waves from cosmological phase transitions*, *JCAP* **04** (2016) 001, [[arXiv:1512.06239](#)].
- [161] M. Hindmarsh, *Sound shell model for acoustic gravitational wave production at a first-order phase transition in the early Universe*, *Phys. Rev. Lett.* **120** (2018), no. 7 071301, [[arXiv:1608.04735](#)].
- [162] J. Jaeckel, V. V. Khoze, and M. Spannowsky, *Hearing the signal of dark sectors with gravitational wave detectors*, *Phys. Rev. D* **94** (2016), no. 10 103519, [[arXiv:1602.03901](#)].
- [163] M. Hindmarsh, S. J. Huber, K. Rummukainen, and D. J. Weir, *Shape of the acoustic gravitational wave power spectrum from a first order phase transition*, *Phys. Rev. D* **96** (2017), no. 10 103520, [[arXiv:1704.05871](#)]. [Erratum: *Phys.Rev.D* 101, 089902 (2020)].
- [164] W.-Y. Ai, B. Laurent, and J. van de Vis, *Model-independent bubble wall velocities in local thermal equilibrium*, *JCAP* **07** (2023) 002, [[arXiv:2303.10171](#)].
- [165] J. Ellis, M. Lewicki, J. M. No, and V. Vaskonen, *Gravitational wave energy budget in strongly supercooled phase transitions*, *JCAP* **06** (2019) 024, [[arXiv:1903.09642](#)].